Correlations and experiment

- Summary of some Green's function results
- Survey of perturbation expansion (very sketchy)
- Discussion of different experimental data

Sp propagator in many-body system

- Similar definition as in sp problem (see preliminary notes)
- Also very useful both for discrete and continuum problems
- Fermion definition

$$G(\alpha,\beta;t-t') = -\frac{i}{\hbar}\langle\Psi_0^N|\,\mathcal{T}[a_{\alpha_H}(t)a^\dagger_{\beta_H}(t')]\,|\Psi_0^N\rangle$$

- with normalized Heisenberg ground state

$$\hat{H}\,|\Psi_0^N\rangle = E_0^N\,|\Psi_0^N\rangle$$

- Heisenberg picture operators

$$a_{\alpha_H}(t) = e^{\frac{i}{\hbar}\hat{H}t}a_\alpha e^{-\frac{i}{\hbar}\hat{H}t}$$

$$a^\dagger_{\alpha_H}(t) = e^{\frac{i}{\hbar}\hat{H}t}a^\dagger_\alpha e^{-\frac{i}{\hbar}\hat{H}t}$$

- and time-ordering operation is defined according to (fermions)

$$\mathcal{T}[a_{\alpha_H}(t)a^\dagger_{\beta_H}(t')] \equiv \theta(t-t')a_{\alpha_H}(t)a^\dagger_{\beta_H}(t') - \theta(t'-t)a^\dagger_{\beta_H}(t')a_{\alpha_H}(t)$$

Use definitions

- Write in detail

$$G(\alpha,\beta;t-t') = -\frac{i}{\hbar}\left\{\theta(t-t')e^{\frac{i}{\hbar}E_0^N(t-t')}\left\langle\Psi_0^N\right| a_\alpha e^{-\frac{i}{\hbar}\hat{H}(t-t')}a_\beta^\dagger\left|\Psi_0^N\right\rangle\right.$$

$$\left. -\theta(t'-t)e^{\frac{i}{\hbar}E_0^N(t'-t)}\left\langle\Psi_0^N\right| a_\beta^\dagger e^{-\frac{i}{\hbar}\hat{H}(t'-t)}a_\alpha\left|\Psi_0^N\right\rangle\right\}$$

$$= -\frac{i}{\hbar}\left\{\theta(t-t')\sum_m e^{\frac{i}{\hbar}(E_0^N-E_m^{N+1})(t-t')}\left\langle\Psi_0^N\right| a_\alpha\left|\Psi_m^{N+1}\right\rangle\left\langle\Psi_m^{N+1}\right| a_\beta^\dagger\left|\Psi_0^N\right\rangle\right.$$

$$\left. -\theta(t'-t)\sum_n e^{\frac{i}{\hbar}(E_0^N-E_n^{N-1})(t'-t)}\left\langle\Psi_0^N\right| a_\beta^\dagger\left|\Psi_n^{N-1}\right\rangle\left\langle\Psi_n^{N-1}\right| a_\alpha\left|\Psi_0^N\right\rangle\right\}$$

- introducing appropriate completeness relations with exact eigenstates

$$\hat{H}\left|\Psi_m^{N+1}\right\rangle = E_m^{N+1}\left|\Psi_m^{N+1}\right\rangle$$

$$\hat{H}\left|\Psi_n^{N-1}\right\rangle = E_n^{N-1}\left|\Psi_n^{N-1}\right\rangle$$

Lehmann representation

- Introduce FT for practical applications

$$G(\alpha,\beta;E) = \int_{-\infty}^{\infty} d(t-t')\; e^{\frac{i}{\hbar}E(t-t')}\; G(\alpha,\beta;t-t')$$

- Use integral representation of step function

$$\begin{aligned} G(\alpha,\beta;E) &= \sum_m \frac{\langle \Psi_0^N | a_\alpha | \Psi_m^{N+1}\rangle \langle \Psi_m^{N+1} | a_\beta^\dagger | \Psi_0^N\rangle}{E-(E_m^{N+1}-E_0^N)+i\eta} \\ &+ \sum_n \frac{\langle \Psi_0^N | a_\beta^\dagger | \Psi_n^{N-1}\rangle \langle \Psi_n^{N-1} | a_\alpha | \Psi_0^N\rangle}{E-(E_0^N-E_n^{N-1})-i\eta} \\ &= \langle \Psi_0^N | a_\alpha \frac{1}{E-(\hat{H}-E_0^N)+i\eta} a_\beta^\dagger | \Psi_0^N\rangle \\ &+ \langle \Psi_0^N | a_\beta^\dagger \frac{1}{E-(E_0^N-\hat{H})-i\eta} a_\alpha | \Psi_0^N\rangle \end{aligned}$$

- Any single-particle basis can be used
- Still “wave functions” and eigenvalues as in sp problem!!

Spectral functions

- Physics of knock-out experiments to be discussed shortly can be interpreted nicely using spectral functions
- For the removal of particles, we have the hole spectral function

$$\begin{aligned} S_h(\alpha;E) &= \frac{1}{\pi}\,\mathrm{Im}\,G(\alpha,\alpha;E) \qquad E \le \varepsilon_F^- \\ &= \sum_n \left| \langle \Psi_n^{N-1} | \, a_\alpha \, | \Psi_0^N \rangle \right|^2 \delta(E - (E_0^N - E_n^{N-1})) \end{aligned}$$

- with $\varepsilon_F^- = E_0^N - E_0^{N-1}$
- A similar addition probability density is available for adding particles (particle spectral function)

$$\begin{aligned} S_p(\alpha;E) &= -\frac{1}{\pi}\,\mathrm{Im}\,G(\alpha,\alpha;E) \qquad E \ge \varepsilon_F^+ \\ &= \sum_m \left| \langle \Psi_m^{N+1} | \, a_\alpha^\dagger \, | \Psi_0^N \rangle \right|^2 \delta(E - (E_m^{N+1} - E_0^N)) \end{aligned}$$

$$\varepsilon_F^+ = E_0^{N+1} - E_0^N$$

$$\frac{1}{E \pm i\eta} = \mathcal{P}\frac{1}{E} \mp i\pi\delta(E)$$

Occupation and depletion

- Occupation number

$$
\begin{aligned}
n(\alpha) &= \langle \Psi_0^N | \, a_\alpha^\dagger a_\alpha \, | \Psi_0^N \rangle = \sum_n \left| \langle \Psi_n^{N-1} | \, a_\alpha \, | \Psi_0^N \rangle \right|^2 \\
&= \int_{-\infty}^{\varepsilon_F^-} dE \; \sum_n \left| \langle \Psi_n^{N-1} | \, a_\alpha \, | \Psi_0^N \rangle \right|^2 \delta(E - (E_0^N - E_n^{N-1})) \\
&= \int_{-\infty}^{\varepsilon_F^-} dE \; S_h(\alpha; E)
\end{aligned}
$$

- Depletion

$$
\begin{aligned}
d(\alpha) &= \langle \Psi_0^N | \, a_\alpha a_\alpha^\dagger \, | \Psi_0^N \rangle = \sum_m \left| \langle \Psi_m^{N+1} | \, a_\alpha^\dagger \, | \Psi_0^N \rangle \right|^2 \\
&= \int_{\varepsilon_F^+}^{\infty} dE \; \sum_m \left| \langle \Psi_m^{N+1} | \, a_\alpha^\dagger \, | \Psi_0^N \rangle \right|^2 \delta(E - (E_m^{N+1} - E_0^N)) \\
&= \int_{\varepsilon_F^+}^{\infty} dE \; S_p(\alpha; E)
\end{aligned}
$$

- Obvious sum rule

$$
n(\alpha) + d(\alpha) = \langle \Psi_0^N | \, a_\alpha^\dagger a_\alpha \, | \Psi_0^N \rangle + \langle \Psi_0^N | \, a_\alpha a_\alpha^\dagger \, | \Psi_0^N \rangle = \langle \Psi_0^N | \Psi_0^N \rangle = 1
$$

Expectation values of operators in ground state

- Consider one-body operator

$$\langle \Psi_0^N | \hat{O} | \Psi_0^N \rangle = \sum_{\alpha,\beta} \langle \alpha | O | \beta \rangle \langle \Psi_0^N | a_\alpha^\dagger a_\beta | \Psi_0^N \rangle = \sum_{\alpha,\beta} \langle \alpha | O | \beta \rangle \, n_{\alpha\beta}$$

- One-body density matrix element $\quad n_{\alpha\beta} \equiv \langle \Psi_0^N | a_\alpha^\dagger a_\beta | \Psi_0^N \rangle$
- can be obtained from sp propagator

$$\begin{aligned} n_{\beta\alpha} &= \int \frac{dE}{2\pi i} \, e^{iE\eta} \, G(\alpha,\beta;E) \\ &= \int \frac{dE}{2\pi i} e^{iE\eta} \sum_m \frac{\langle \Psi_0^A | a_\alpha | \Psi_m^{A+1} \rangle \langle \Psi_m^{A+1} | a_\beta^\dagger | \Psi_0^A \rangle}{E - (E_m^{A+1} - E_0^A) + i\eta} \\ &+ \int \frac{dE}{2\pi i} \, e^{iE\eta} \, \sum_n \frac{\langle \Psi_0^N | a_\beta^\dagger | \Psi_n^{N-1} \rangle \langle \Psi_n^{N-1} | a_\alpha | \Psi_0^N \rangle}{E - (E_0^N - E_n^{N-1}) - i\eta} \\ &= \sum_n \langle \Psi_0^N | a_\beta^\dagger | \Psi_n^{N-1} \rangle \langle \Psi_n^{N-1} | a_\alpha | \Psi_0^N \rangle = \langle \Psi_0^N | a_\beta^\dagger a_\alpha | \Psi_0^N \rangle \end{aligned}$$

- or $\quad n_{\beta\alpha} = \frac{1}{\pi} \int_{-\infty}^{\varepsilon_F^-} dE \;\; \mathrm{Im}\, G(\alpha,\beta;E) = \langle \Psi_0^N | a_\beta^\dagger a_\alpha | \Psi_0^N \rangle$

Magic?!: energy sum rule

- Consider

$$\begin{aligned} I_\alpha &= \frac{1}{\pi}\int_{-\infty}^{\varepsilon_F^-} dE\ E\ \ \mathrm{Im}\ G(\alpha,\alpha;E) = \int_{-\infty}^{\varepsilon_F^-} dE\ E\ S_h(\alpha;E) \\ &= \sum_m (E_0^N - E_m^{N-1}) \langle \Psi_0^N | a_\alpha^\dagger | \Psi_m^{N-1} \rangle \langle \Psi_m^{N-1} | a_\alpha | \Psi_0^N \rangle \\ &= \langle \Psi_0^N | a_\alpha^\dagger a_\alpha \hat{H} | \Psi_0^N \rangle - \sum_m \langle \Psi_0^N | a_\alpha^\dagger E_m^{N-1} | \Psi_m^{N-1} \rangle \langle \Psi_m^{N-1} | a_\alpha | \Psi_0^N \rangle \\ &= \langle \Psi_0^N | a_\alpha^\dagger a_\alpha \hat{H} | \Psi_0^N \rangle - \langle \Psi_0^N | a_\alpha^\dagger \hat{H} a_\alpha | \Psi_0^N \rangle = \langle \Psi_0^N | a_\alpha^\dagger [a_\alpha, \hat{H}] | \Psi_0^N \rangle \end{aligned}$$

- Earlier results yield $[a_\alpha, \hat{H}] = \sum_\beta \langle \alpha | T | \beta \rangle a_\beta + \sum_{\beta\gamma\delta} (\alpha\beta|V|\gamma\delta) a_\beta^\dagger a_\delta a_\gamma$

- Insert $I_\alpha = \sum_\beta \langle \alpha | T | \beta \rangle \langle \Psi_0^N | a_\alpha^\dagger a_\beta | \Psi_0^N \rangle + \sum_{\beta\gamma\delta} (\alpha\beta|V|\gamma\delta)\ \langle \Psi_0^N | a_\alpha^\dagger a_\beta^\dagger a_\delta a_\gamma | \Psi_0^N \rangle$

- Sum over α

$$\sum_\alpha I_\alpha = \langle \Psi_0^N | \hat{T} | \Psi_0^N \rangle + 2 \langle \Psi_0^N | \hat{V} | \Psi_0^N \rangle$$

Galitski-Migdal energy sum rule (Koltun)

- Combine with half the expectation value of the kinetic energy

$$
\begin{aligned}
E_0^N &= \langle \Psi_0^N | \hat{H} | \Psi_0^N \rangle \\
&= \frac{1}{2\pi} \int_{-\infty}^{\varepsilon_F^-} dE \sum_{\alpha,\beta} \{ \langle \alpha | T | \beta \rangle + E \, \delta_{\alpha,\beta} \} \; \mathrm{Im}\, G(\beta, \alpha; E) \\
&= \frac{1}{2} \left(\sum_{\alpha,\beta} \langle \alpha | T | \beta \rangle \, n_{\alpha\beta} + \sum_{\alpha} \int_{-\infty}^{\varepsilon_F^-} dE \; E \; S_h(\alpha; E) \right)
\end{aligned}
$$

- complete result only when there are no three- or higher-body interactions
- sp propagator (hole part) yields energy of the ground state
- later: particle part yields elastic scattering cross section

Noninteracting propagator

- Propagator for $\hat{H}_0$ involves interaction picture

$$G^{(0)}(\alpha,\beta;t-t') = -\frac{i}{\hbar}\langle\Phi_0^N|\,\mathcal{T}[a_{\alpha_I}(t)a^\dagger_{\beta_I}(t')]\,|\Phi_0^N\rangle$$

- with corresponding ground state

$$\hat{H}_0\,|\Phi_0^N\rangle = E_{\Phi_0^N}\,|\Phi_0^N\rangle$$

$$E_{\Phi_0^N} = \sum_{\alpha<F}\varepsilon_\alpha$$

- as for IPM so closed-shell atom or nucleus for example
- Operators $\quad a_{\alpha_I}(t) = e^{\frac{i}{\hbar}\hat{H}_0 t}a_\alpha e^{-\frac{i}{\hbar}\hat{H}_0 t} = e^{-i\varepsilon_\alpha t/\hbar}a_\alpha$

$$a^\dagger_{\alpha_I}(t) = e^{\frac{i}{\hbar}\hat{H}_0 t}a^\dagger_\alpha e^{-\frac{i}{\hbar}\hat{H}_0 t} = e^{i\varepsilon_\alpha t/\hbar}a^\dagger_\alpha$$

- assuming $\hat{H}_0$ is diagonal in this basis

Evaluate noninteracting sp propagator

- Insert

$$G^{(0)}(\alpha,\beta;t-t') = G_+^{(0)}(\alpha,\beta;t-t') + G_-^{(0)}(\alpha,\beta;t-t')$$

$$= -\frac{i}{\hbar}\delta_{\alpha\beta}\{\theta(t-t')\theta(\alpha-F)e^{-\frac{i}{\hbar}\varepsilon_\alpha(t-t')} - \theta(t'-t)\theta(F-\alpha)e^{\frac{i}{\hbar}\varepsilon_\alpha(t'-t)}\}$$

- propagation of a particle or a hole on top of noninteracting ground state

- directly:

$$\hat{H}_0\; a_\alpha^\dagger \left|\Phi_0^N\right\rangle = \left(E_{\Phi_0^N} + \varepsilon_\alpha\right)\, a_\alpha^\dagger \left|\Phi_0^N\right\rangle \qquad \alpha > F$$

$$\hat{H}_0\; a_\alpha \left|\Phi_0^N\right\rangle = \left(E_{\Phi_0^N} - \varepsilon_\alpha\right)\, a_\alpha \left|\Phi_0^N\right\rangle \qquad \alpha < F$$

- FT

$$G^{(0)}(\alpha,\beta;E) = \delta_{\alpha,\beta}\left\{\frac{\theta(\alpha-F)}{E-\varepsilon_\alpha+i\eta} + \frac{\theta(F-\alpha)}{E-\varepsilon_\alpha-i\eta}\right\}$$

Noninteracting spectral functions

- Imaginary parts yield all the strength at one location

$$\begin{aligned} S_h^{(0)}(\alpha;E) &= \frac{1}{\pi}\text{Im } G^{(0)}(\alpha,\alpha;E) & E < \varepsilon_F^{(0)^-} \\ &= \delta(E-\varepsilon_\alpha)\ \theta(F-\alpha) \\ S_p^{(0)}(\alpha;E) &= -\frac{1}{\pi}\text{Im } G^{(0)}(\alpha,\alpha;E) & E > \varepsilon_F^{(0)^+} \\ &= \delta(E-\varepsilon_\alpha)\ \theta(\alpha-F) \end{aligned}$$

- in this basis: either completely full or empty

$$n^{(0)}(\alpha) = \int_{-\infty}^{\varepsilon_F^{(0)^-}} dE\ \delta(E-\varepsilon_\alpha)\ \theta(F-\alpha) = \theta(F-\alpha)$$

- other basis $G^{(0)}(\boldsymbol{r}m_s,\boldsymbol{r}'m_s';E) = \langle\Phi_0^N|\, a_{\boldsymbol{r}m_s} \dfrac{1}{E-(\hat{H}_0 - E_{\Phi_0^N}) + i\eta} a^\dagger_{\boldsymbol{r}'m_s'}\,|\Phi_0^N\rangle$

$$+ \langle\Phi_0^N|\, a^\dagger_{\boldsymbol{r}'m_s'} \frac{1}{E-(E_{\Phi_0^N} - \hat{H}_0) - i\eta} a_{\boldsymbol{r}m_s}\,|\Phi_0^N\rangle$$

$$= \sum_\alpha \left\{ \frac{\langle \boldsymbol{r}m_s|\alpha\rangle\langle\alpha|\boldsymbol{r}'m_s'\rangle\theta(\alpha-F)}{E-\varepsilon_\alpha+i\eta} + \frac{\langle \boldsymbol{r}m_s|\alpha\rangle\langle\alpha|\boldsymbol{r}'m_s'\rangle\theta(F-\alpha)}{E-\varepsilon_\alpha-i\eta} \right\}$$

Link between interacting and noninteracting propagator

- Define $|\Psi_I(t)\rangle = \exp\left\{\frac{i}{\hbar}\hat{H}_0 t\right\}|\Psi_S(t)\rangle$ to obtain $i\hbar\frac{\partial}{\partial t}|\Psi_I(t)\rangle = \hat{H}_1(t)\,|\Psi_I(t)\rangle$
- with $\hat{H} = \hat{H}_0 + \hat{H}_1$ and $\hat{O}_I(t) = \exp\left\{\frac{i}{\hbar}\hat{H}_0 t\right\}\hat{O}_S \exp\left\{-\frac{i}{\hbar}\hat{H}_0 t\right\}$
- Define $|\Psi_I(t)\rangle = \hat{\mathcal{U}}(t,t_0)\,|\Psi_I(t_0)\rangle$ time evolution in the interaction picture
- It follows that $i\hbar\frac{\partial}{\partial t}|\Psi_I(t)\rangle = \hat{H}_1(t)\,|\Psi_I(t)\rangle$
- Iterate and analyze:

$$\hat{\mathcal{U}}(t,t_0) = \sum_{n=0}^{\infty}\left(\frac{-i}{\hbar}\right)^n \frac{1}{n!}\int_{t_0}^{t} dt_1 \int_{t_0}^{t} dt_2 ... \int_{t_0}^{t} dt_n \;\mathcal{T}\left[\hat{H}_1(t_1)\hat{H}_1(t_2)...\hat{H}_1(t_n)\right]$$

- Explicit construction

$$\hat{\mathcal{U}}(t,t_0) = \exp\left\{\frac{i}{\hbar}\hat{H}_0 t\right\}\exp\left\{-\frac{i}{\hbar}\hat{H}(t-t_0)\right\}\exp\left\{-\frac{i}{\hbar}\hat{H}_0 t_0\right\}$$

- Insert in propagator and include cancellation of terms —> diagrams with Wick's theorem (see DVN Ch.8)

$$G(\alpha,\beta;t-t') = -\frac{i}{\hbar}\sum_{m}^{\infty}\left(\frac{-i}{\hbar}\right)^m \frac{1}{m!}\int dt_1 .. \int dt_m \,\langle\Phi_0^N|\,\mathcal{T}\left[\hat{H}_1(t_1)..\hat{H}_1(t_m)a_\alpha(t)a_\beta^\dagger(t')\right]|\Phi_0^N\rangle_{connected}$$

- Each term in the expansion can be uniquely identified with a Feynman diagram
- Small set of rules allow for complete graphical depiction that helps in visualizing the expansion

Strategy

- Go from $\mathcal{T}$ to N
- Theorem $\mathcal{T}\left[\hat{a}\hat{b}\hat{c}...\hat{x}\hat{y}\hat{z}\right] = N\left[\hat{a}\hat{b}\hat{c}...\hat{x}\hat{y}\hat{z}\right] + N\left[\hat{a}^{\bullet}\hat{b}^{\bullet}\hat{c}...\hat{x}\hat{y}\hat{z}\right] + N\left[\hat{a}^{\bullet}\hat{b}\hat{c}^{\bullet}...\hat{x}\hat{y}\hat{z}\right]$

$$+ ... + N\left[\hat{a}^{\bullet}\hat{b}\hat{c}...\hat{x}\hat{y}\hat{z}^{\bullet}\right] + N\left[\hat{a}\hat{b}^{\bullet}\hat{c}^{\bullet}...\hat{x}\hat{y}\hat{z}\right] + ... + N\left[\hat{a}^{\bullet}\hat{b}^{\bullet\bullet}\hat{c}...^{\bullet}...^{\bullet\bullet}\hat{x}\hat{y}\hat{z}\right]$$

★

$$+ ... + N\left[\hat{a}^{\bullet}\hat{b}^{\bullet\bullet}\hat{c}^{\bullet\bullet\bullet}...\hat{x}^{\circ}\hat{y}^{\circ\circ}\hat{z}^{\circ\circ\circ}\right]$$

$$= N\left[\hat{a}\hat{b}\hat{c}...\hat{x}\hat{y}\hat{z}\right] + N\left[\text{sum over all possible pairs of contractions}\right]$$

- only fully contracted contributions survive when expectation value with respect to $|\Phi_0^N\rangle$ is taken!
- Use fermion sign convention also for normal ordering
- Each contraction $a_\alpha(t)^{\bullet} a_\beta^\dagger(t')^{\bullet} = i\hbar\, G^{(0)}(\alpha, \beta; t - t')$ for all quantum numbers and time orderings —> Feynman diagrams

Diagram rules (time-dependent version)

- Assume auxiliary potential absent; then for $\hat{V}^m$
- Rules

Rule 1 Draw all topologically distinct and connected diagrams with m horizontal interaction lines for V (dashed) and $2m+1$ directed (using arrows) Green's functions $G^{(0)}$

Rule 2 Label external points appropriately. For example, the labels α, t and β, t' apply for Eq. (8.55)
Label each interaction with a time and sp quantum numbers

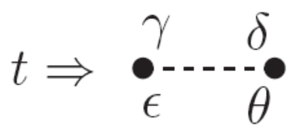

$$\Rightarrow \quad (\gamma\delta|V|\epsilon\theta)$$

For each full line one writes

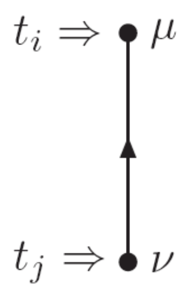

$$\Rightarrow \quad G^{(0)}(\mu, \nu; t_i - t_j)$$

Rule 3 Sum (integrate) over all internal sp quantum numbers and integrate over all m internal times

Rule 4 Include a factor $(i\hbar)^m$ and $(-1)^F$ where F is the number of closed fermion loops

Rule 5 Interpret equal times in a propagator as $G^{(0)}(\mu, \nu; t - t^+)$

Interpretation

- Unclear about topological equivalence: resort to Wick's theorem
- Fermion lines run continuously from the external label α to β or form closed loops
- A closed loop yields a minus sign
- Contractions for a loop will look like

$$a^\dagger(t_1)^\bullet a(t_1)^{\bullet\bullet} a^\dagger(t_2)^{\bullet\bullet} a(t_2)^\circ \ldots a^\dagger(t_m)^{\circ\circ} a(t_m)^\bullet$$

- requires one additional sign to contract first and last operator

$$(i\hbar)^m = -\frac{i}{\hbar} \times \left(-\frac{i}{\hbar}\right)^m \times (i\hbar)^{2m+1}$$

- = prefactor X factor under sum X # of contractions in mth order
- Drawing of diagrams emphasizes static nature of interaction

First-order terms

- Use rules

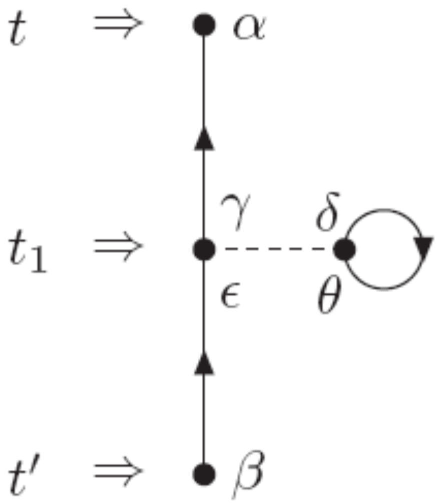

$$\Rightarrow (-1)\ i\hbar \int dt_1 \ \sum_{\gamma\delta\epsilon\theta} (\gamma\delta|V|\epsilon\theta)\, G^{(0)}(\alpha,\gamma;t-t_1)$$
$$\times\ G^{(0)}(\theta,\delta;t_1-t_1^+)G^{(0)}(\epsilon,\beta;t_1-t')$$

- Diagram V1D

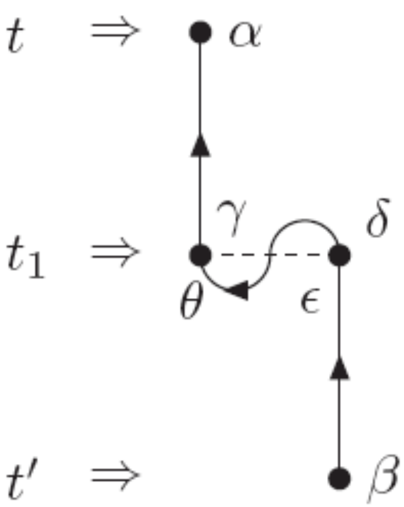

$$\Rightarrow i\hbar \int dt_1 \ \sum_{\gamma\delta\epsilon\theta} (\gamma\delta|V|\theta\epsilon)\, G^{(0)}(\alpha,\gamma;t-t_1)$$
$$\times\ G^{(0)}(\theta,\delta;t_1-t_1^+)G^{(0)}(\epsilon,\beta;t_1-t')$$

- Diagram V1E

Second-order terms

- V2a

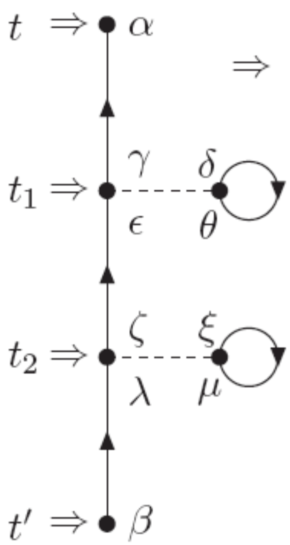

$$\Rightarrow (-1)^2(i\hbar)^2 \int dt_1 \int dt_2 \sum_{\gamma,\delta,\epsilon,\theta} \sum_{\zeta,\xi,\lambda,\mu} G^{(0)}(\alpha,\gamma;t-t_1)$$
$$\times\ (\gamma\delta|V|\epsilon\theta)\, G^{(0)}(\epsilon,\zeta;t_1-t_2)G^{(0)}(\theta,\delta;t_1-t_1^+)$$
$$\times\ G^{(0)}(\mu,\xi;t_2-t_2^+)\,(\zeta\xi|V|\lambda\mu)\,G^{(0)}(\lambda,\beta;t_2-t')$$

- V2b

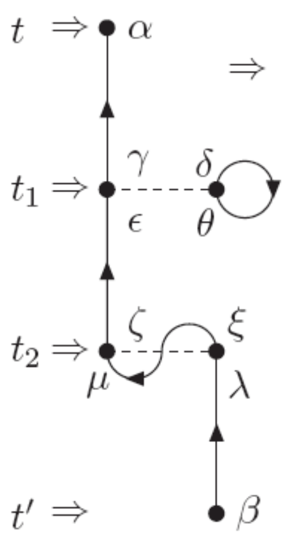

$$\Rightarrow (-1)(i\hbar)^2 \int dt_1 \int dt_2 \sum_{\gamma,\delta,\epsilon,\theta} \sum_{\zeta,\xi,\lambda,\mu} G^{(0)}(\alpha,\gamma;t-t_1)$$
$$\times\ (\gamma\delta|V|\epsilon\theta)\, G^{(0)}(\epsilon,\zeta;t_1-t_2)G^{(0)}(\theta,\delta;t_1-t_1^+)$$
$$\times\ G^{(0)}(\mu,\xi;t_2-t_2^+)\,(\zeta\xi|V|\mu\lambda)\,G^{(0)}(\lambda,\beta;t_2-t')$$

more

- V2c

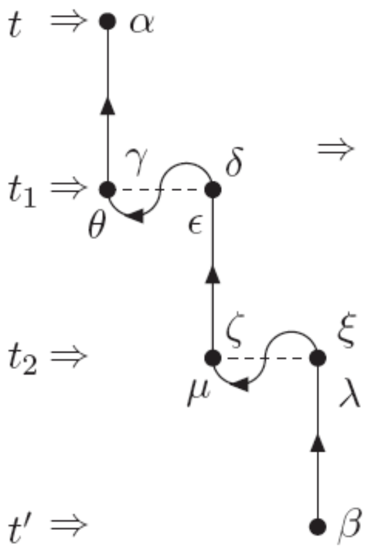

$$\Rightarrow (i\hbar)^2 \int dt_1 \int dt_2 \sum_{\gamma,\delta,\epsilon,\theta} \sum_{\zeta,\xi,\lambda,\mu} G^{(0)}(\alpha,\gamma;t-t_1)$$
$$\times\ (\gamma\delta|V|\theta\epsilon)\, G^{(0)}(\epsilon,\zeta;t_1-t_2) G^{(0)}(\theta,\delta;t_1-t_1^+)$$
$$\times\ G^{(0)}(\mu,\xi;t_2-t_2^+)\,(\zeta\xi|V|\mu\lambda)\, G^{(0)}(\lambda,\beta;t_2-t')$$

- V2d

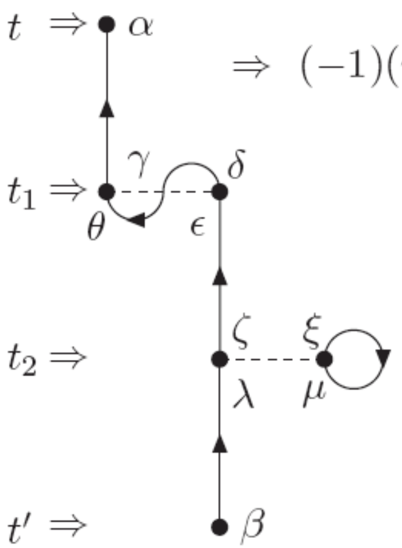

$$\Rightarrow (-1)(i\hbar)^2 \int dt_1 \int dt_2 \sum_{\gamma,\delta,\epsilon,\theta} \sum_{\zeta,\xi,\lambda,\mu} G^{(0)}(\alpha,\gamma;t-t_1)$$
$$\times\ (\gamma\delta|V|\theta\epsilon)\, G^{(0)}(\epsilon,\zeta;t_1-t_2) G^{(0)}(\theta,\delta;t_1-t_1^+)$$
$$\times\ G^{(0)}(\mu,\xi;t_2-t_2^+)\,(\zeta\xi|V|\lambda\mu)\, G^{(0)}(\lambda,\beta;t_2-t')$$

and more

- **V2e**

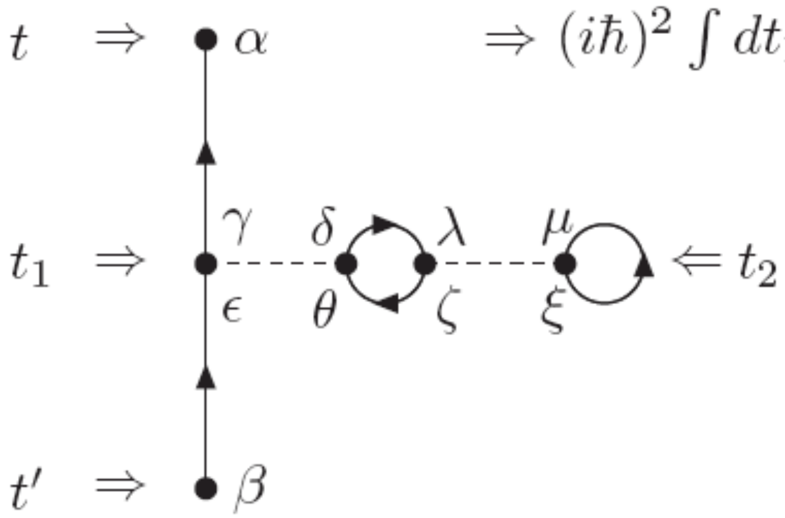

$$\Rightarrow (i\hbar)^2 \int dt_1 \int dt_2 \sum_{\gamma\delta\epsilon\theta} \sum_{\zeta\xi\lambda\mu} G^{(0)}(\alpha,\gamma;t-t_1)$$
$$\times\ (\gamma\delta|V|\epsilon\theta)\, G^{(0)}(\lambda,\delta;t_2-t_1)$$
$$\times\ G^{(0)}(\theta,\zeta;t_1-t_2)\,(\zeta\xi|V|\lambda\mu)$$
$$\times\ G^{(0)}(\mu,\xi;t_2-t_2^+)G^{(0)}(\epsilon,\beta;t_1-t')$$

- **V2f**

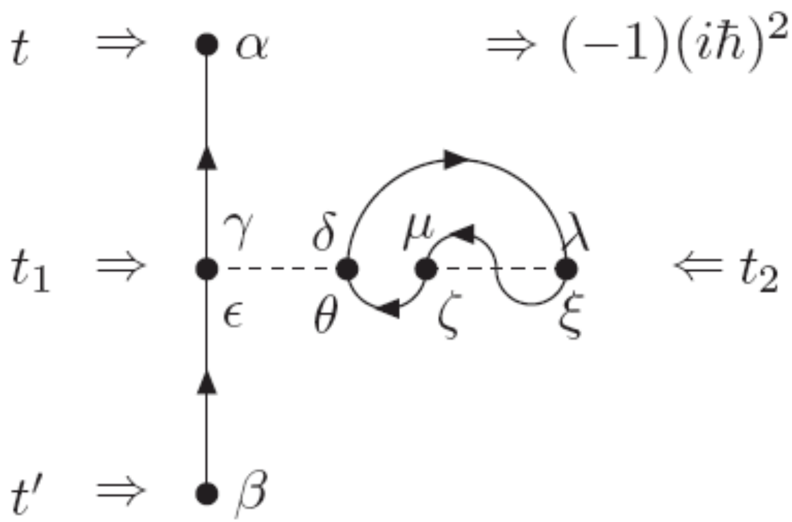

$$\Rightarrow (-1)(i\hbar)^2 \int dt_1 \int dt_2 \sum_{\gamma\delta\epsilon\theta} \sum_{\zeta\xi\lambda\mu} G^{(0)}(\alpha,\gamma;t-t_1)$$
$$\times\ (\gamma\delta|V|\epsilon\theta)\, G^{(0)}(\lambda,\delta;t_2-t_1)$$
$$\times\ G^{(0)}(\theta,\zeta;t_1-t_2)\,(\xi\zeta|V|\lambda\mu)$$
$$\times\ G^{(0)}(\mu,\xi;t_2-t_2^+)G^{(0)}(\epsilon,\beta;t_1-t')$$

and more ...

- V2g

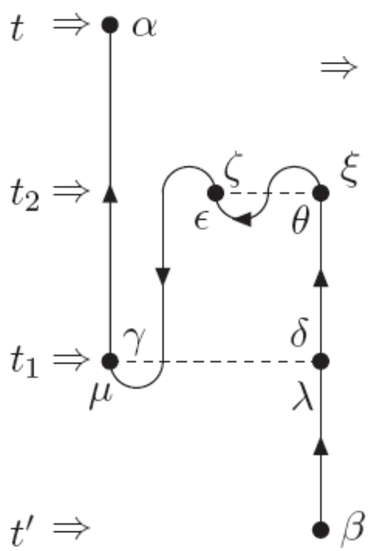

$$\Rightarrow (i\hbar)^2 \int dt_1 \int dt_2 \sum_{\gamma,\delta,\lambda,\mu} \sum_{\zeta,\xi,\epsilon,\theta} G^{(0)}(\alpha,\gamma;t-t_1)$$
$$\times\ (\gamma\delta|V|\mu\lambda)\, G^{(0)}(\mu,\zeta;t_1-t_2)$$
$$\times\ G^{(0)}(\theta,\delta;t_2-t_1)G^{(0)}(\epsilon,\xi;t_2-t_2^+)$$
$$\times\ (\zeta\xi|V|\epsilon\theta)\, G^{(0)}(\lambda,\beta;t_1-t')$$

- V2h

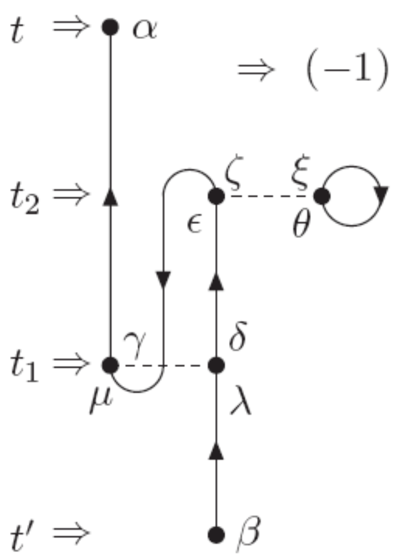

$$\Rightarrow (-1)(i\hbar)^2 \int dt_1 \int dt_2 \sum_{\gamma,\delta,\lambda,\mu} \sum_{\zeta,\xi,\epsilon,\theta} G^{(0)}(\alpha,\gamma;t-t_1)$$
$$\times\ (\gamma\delta|V|\mu\lambda)\, G^{(0)}(\mu,\zeta;t_1-t_2)$$
$$\times\ G^{(0)}(\epsilon,\delta;t_2-t_1)G^{(0)}(\theta,\xi;t_2-t_2^+)$$
$$\times\ (\zeta\xi|V|\epsilon\theta)\, G^{(0)}(\lambda,\beta;t_1-t')$$

and finally

- V2i

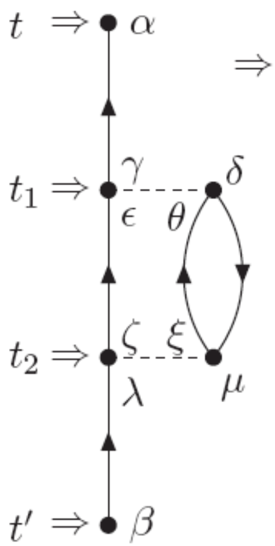

$$\Rightarrow (-1)(i\hbar)^2 \int dt_1 \int dt_2 \sum_{\gamma,\delta,\epsilon,\theta} \sum_{\zeta,\xi,\lambda,\mu} G^{(0)}(\alpha,\gamma;t-t_1)$$
$$\times\ (\gamma\delta|V|\epsilon\theta)\, G^{(0)}(\epsilon,\zeta;t_1-t_2)$$
$$\times\ G^{(0)}(\mu,\delta;t_2-t_1)G^{(0)}(\theta,\xi;t_1-t_2)$$
$$\times\ (\zeta\xi|V|\lambda\mu)\, G^{(0)}(\lambda,\beta;t_2-t')$$

- V2j

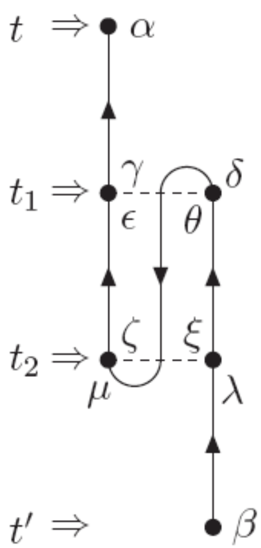

$$\Rightarrow (i\hbar)^2 \int dt_1 \int dt_2 \sum_{\gamma,\delta,\epsilon,\theta} \sum_{\zeta,\xi,\lambda,\mu} G^{(0)}(\alpha,\gamma;t-t_1)$$
$$\times\ (\gamma\delta|V|\epsilon\theta)\, G^{(0)}(\epsilon,\zeta;t_1-t_2)$$
$$\times\ G^{(0)}(\mu,\delta;t_2-t_1)G^{(0)}(\theta,\xi;t_1-t_2)$$
$$\times\ (\zeta\xi|V|\mu\lambda)\, G^{(0)}(\lambda,\beta;t_2-t')$$

Other way of drawing diagrams

- Compare with field-theoretical diagrams (Fetter & Walecka)

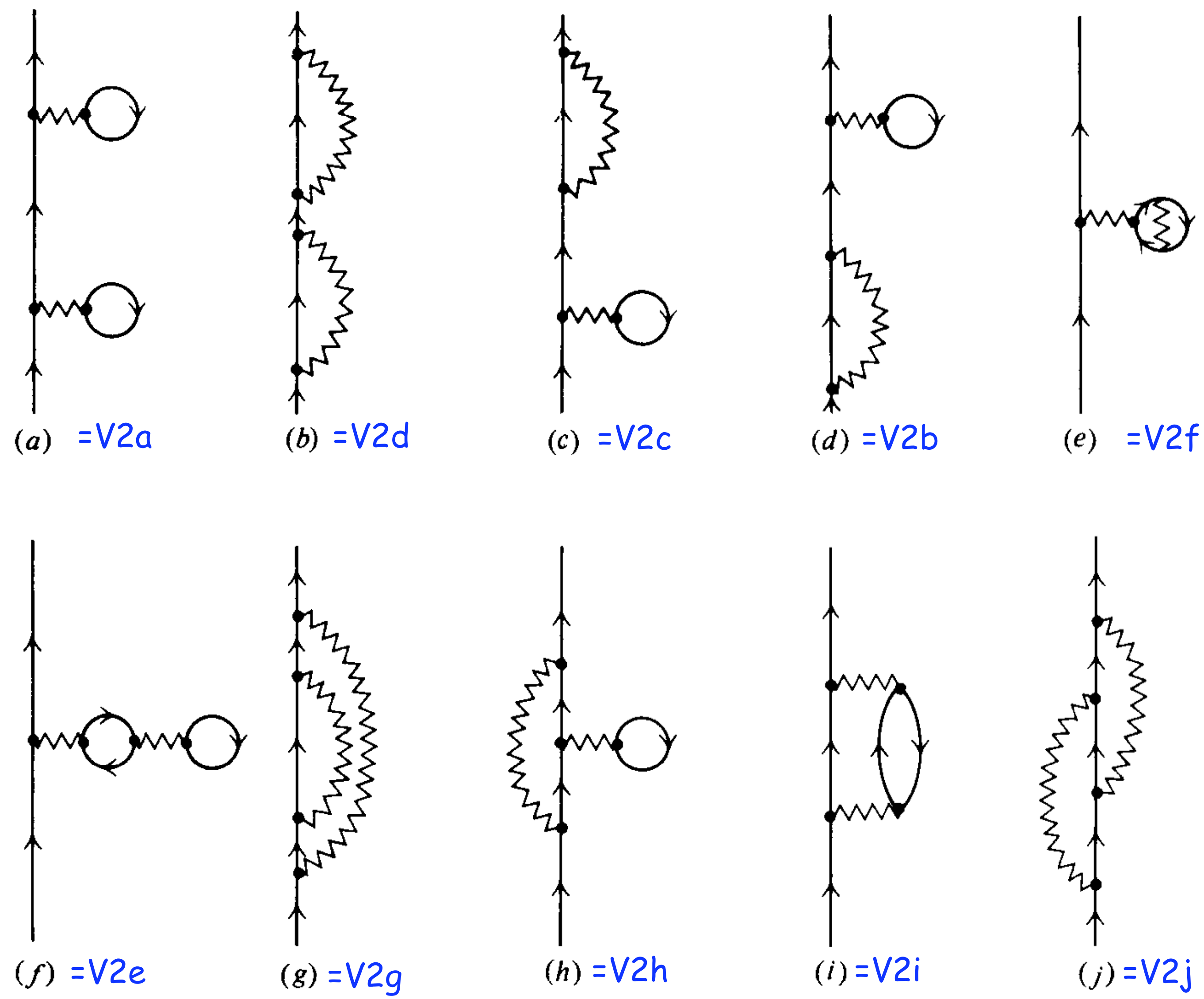

- Topologically the same (use strings or elastics)

Comments

- V2a-V2d iterations of 1st order
- V2e-V2h replace internal propagator by 1st-order one
- V2i-V2j "real" second-order terms (see later applications)
- V2a-V2h summed in mean-field / Hartree-Fock approximation
- Third of higher-order diagrams not often explicitly needed
- Infinite-order summations important but can be generated by manipulating lower-order terms

Include diagrams with auxiliary potential

Rule 6 Label each U according to

$\Rightarrow t_i$

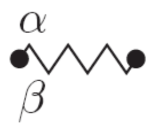

$\Rightarrow \langle\alpha|\, U \,|\beta\rangle$

Rule 7 Include a factor $(-1)^k$ and k additional propagators $G^{(0)}$

$\hat{V} = \frac{1}{2}\sum_{\alpha\beta\gamma\delta}(\alpha\beta|V|\gamma\delta)a_\alpha^\dagger a_\beta^\dagger a_\delta a_\gamma$ also $\hat{V} = \frac{1}{4}\sum_{\alpha\beta\gamma\delta}\langle\alpha\beta|\, V \,|\gamma\delta\rangle\, a_\alpha^\dagger a_\beta^\dagger a_\delta a_\gamma$ with

$$\langle\alpha\beta|\, V \,|\gamma\delta\rangle \equiv (\alpha\beta|V|\gamma\delta) - (\alpha\beta|V|\delta\gamma) = \langle\alpha\beta|\, \hat{V} \,|\gamma\delta\rangle$$

Include direct and exchange terms together

- V2a-V2d only represented by V2a using antisymmetrized matrix elements
- V2e-V2g similarly only by V2e
- V2i-V2j by V2i but requires factor $\frac{1}{2}$ for "equivalent" lines
- For symmetrized diagrams rule change

Rule 1′ Draw only all topologically distinct and connected, direct diagrams with m horizontal interaction lines for V (dashed) and $2m+1$ directed (using arrows) Green's functions $G^{(0)}$

Rule 8 Include a factor $\frac{1}{2}$ for each pair of equivalent lines, which both start at the same interaction and end at another

Energy formulation

- Remember

$$G(\alpha,\beta;E) = \sum_m \frac{\langle\Psi_0^N|\, a_\alpha \,|\Psi_m^{N+1}\rangle \langle\Psi_m^{N+1}|\, a_\beta^\dagger \,|\Psi_0^N\rangle}{E-(E_m^{N+1}-E_0^N)+i\eta} + \sum_n \frac{\langle\Psi_0^N|\, a_\beta^\dagger \,|\Psi_n^{N-1}\rangle \langle\Psi_n^{N-1}|\, a_\alpha \,|\Psi_0^N\rangle}{E-(E_0^N-E_n^{N-1})-i\eta}$$

- Goals:
  - Find eigenvalues

$$\varepsilon_m^+ = E_m^{N+1} - E_0^N$$
$$\varepsilon_n^- = E_0^N - E_n^{N-1}$$

  - and corresponding "wave functions"

$$\mathcal{X}_\beta^m = \langle\Psi_m^{N+1}|\, a_\beta^\dagger \,|\Psi_0^N\rangle$$
$$\mathcal{Y}_\alpha^n = \langle\Psi_n^{N-1}|\, a_\alpha \,|\Psi_0^N\rangle$$

Noninteracting propagator

- Already done

$$G^{(0)}(\alpha,\beta;E) = \int_{-\infty}^{\infty} d(t-t')\ e^{\frac{i}{\hbar}E(t-t')} G^{(0)}(\alpha,\beta;t-t')$$

$$= \delta_{\alpha,\beta}\left\{ \frac{\theta(\alpha-F)}{E-\varepsilon_\alpha+i\eta} + \frac{\theta(F-\alpha)}{E-\varepsilon_\alpha-i\eta} \right\}$$

- Results for expansion of propagator in time formulation employed integration limits $\infty(1-i\eta)$

$-\infty(1-i\eta)$

- Employing $\theta(t-t_0) = -\int \frac{dE'}{2\pi i}\ \frac{e^{-iE'(t-t_0)/\hbar}}{E'+i\eta}$ in noninteracting propagators already eliminates all unwanted contributions (see Mattuck p.40) when the difference between time limits approaches infinity $\Rightarrow$ use integration limits as above

Inverse FT

- Consider $G^{(0)}(\alpha,\beta;\tau) = \int_{-\infty}^{\infty} \frac{dE}{2\pi\hbar}\, e^{-iE\tau/\hbar}\, G^{(0)}(\alpha,\beta;E)$
- Check (do contours)
- Special case of equal-time argument: interpret

$$G^{(0)}(\alpha,\beta;t-t^{+}) = \int_{-\infty}^{\infty} \frac{dE}{2\pi\hbar}\, e^{-iE0^{-}/\hbar}\, G^{(0)}(\alpha,\beta;E)$$
$$= \int_{C\uparrow} \frac{dE}{2\pi\hbar}\, G^{(0)}(\alpha,\beta;E)$$

- $C\uparrow$ contour enclosing the upper half of the complex energy plane
- All diagrams can now be Fourier transformed
- Strategy:
  - for any diagram in time formulation replace noninteracting propagators by above expressions
  - perform time integrations (lots of delta functions)

Changes in energy formulation

- Diagram structure the same topology
- Labels different: unperturbed propagators labeled by energy
- Example clarifies that interaction conserves energy: sum of two incoming energies must combine to sum of two outgoing ones
- Example: V1DE

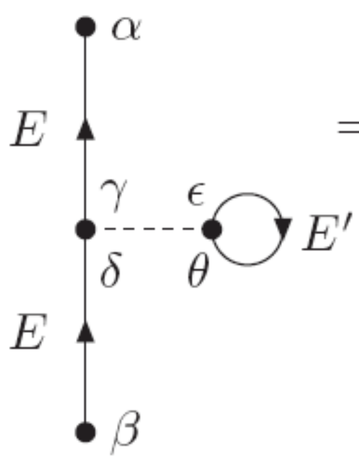

$$\Rightarrow \sum_{\gamma\delta} G^{(0)}(\alpha,\gamma;E)$$
$$\times \; -i\sum_{\epsilon\theta} \langle \gamma\epsilon | V | \delta\theta \rangle \int_{C\uparrow} \frac{dE'}{2\pi} G^{(0)}(\theta,\epsilon;E')$$
$$\times \; G^{(0)}(\delta,\beta;E)$$

- Arrows represent flow of energy
- Only V terms in mth order: m time integrations plus external one, each leading to energy-conserving delta-function (use m+1 factors of $(2\pi\hbar)^{-1}$ from original 2m+1 from inverse FT of $G^{(0)}$)
- With auxiliary potential no factors

Diagram rules in energy formulation (symmetrized)

Rule 1 Draw all topologically distinct (direct) and connected diagrams with m horizontal interaction lines for V (dashed) and $2m+1$ directed (using arrows) Green's functions $G^{(0)}$

Rule 2 Label external points only with sp quantum numbers, *e.g.* α and β

Label each interaction with sp quantum numbers

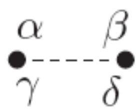

$$\Rightarrow \; \langle\alpha\beta|\,V\,|\gamma\delta\rangle = (\alpha\beta|V|\gamma\delta) - (\alpha\beta|V|\delta\gamma)$$

For each arrow line one writes

$$\Rightarrow \; G^{(0)}(\mu,\nu;E)$$

but in such a way that energy is conserved for each V

Rule 3 Sum (integrate) over all internal sp quantum numbers and integrate over all m internal energies

For each closed loop an independent energy integration occurs over the contour $C\uparrow$

Rule 4 Include a factor $(i/2\pi)^m$ and $(-1)^F$ where F is the number of closed fermion loops

Rule 5 Include a factor of $\frac{1}{2}$ for each equivalent pair of lines

Examples in second order

- V2a

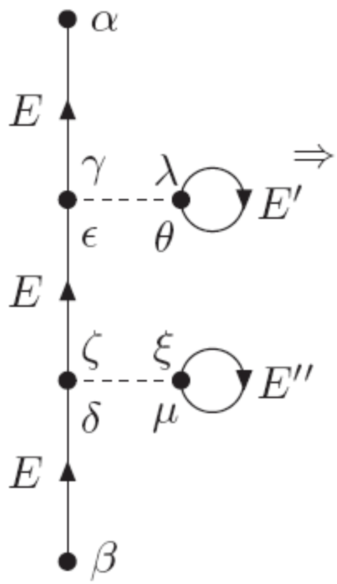

$$\Rightarrow \sum_{\gamma\delta} G^{(0)}(\alpha,\gamma;E)$$
$$\times (-1)^2 i^2 \sum_{\epsilon,\zeta} \sum_{\lambda,\theta} \int_{C\uparrow} \frac{dE'}{2\pi} \langle\gamma\lambda|\, V \,|\epsilon\theta\rangle\, G^{(0)}(\theta,\lambda;E')$$
$$\times G^{(0)}(\epsilon,\zeta;E) \sum_{\xi,\mu} \int_{C\uparrow} \frac{dE''}{2\pi} \langle\zeta\xi|\, V \,|\delta\mu\rangle\, G^{(0)}(\mu,\xi;E'')$$
$$\times G^{(0)}(\delta,\beta;E)$$

- V2e

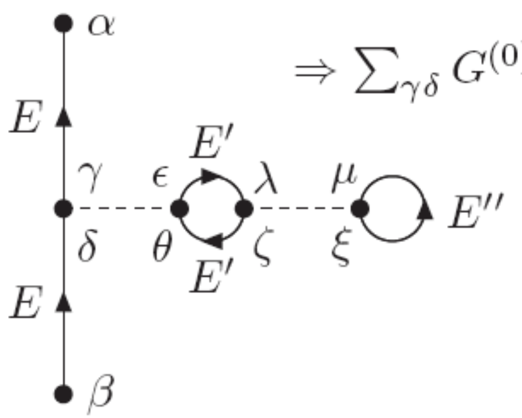

$$\Rightarrow \sum_{\gamma\delta} G^{(0)}(\alpha,\gamma;E) \times\; i^2 \sum_{\epsilon\theta} \sum_{\lambda\zeta} \int_{C\uparrow} \frac{dE'}{2\pi}$$
$$\times \langle\gamma\epsilon|\, V \,|\delta\theta\rangle\, G^{(0)}(\lambda,\epsilon;E') G^{(0)}(\theta,\zeta;E')$$
$$\times \sum_{\mu\xi} \int_{C\uparrow} \frac{dE''}{2\pi} \langle\zeta\xi|\, V \,|\lambda\mu\rangle\, G^{(0)}(\mu,\xi;E'')$$
$$\times G^{(0)}(\delta,\beta;E)$$

Last term

- V2i

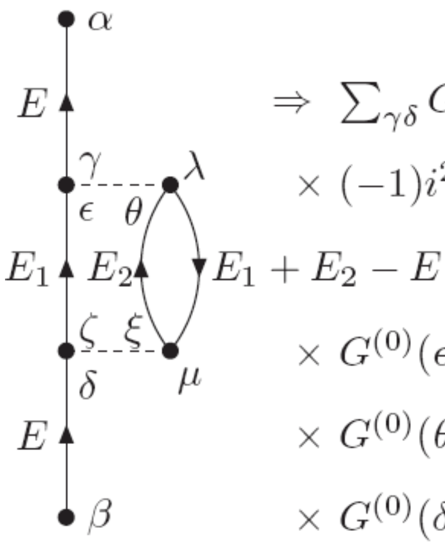

$$\Rightarrow \sum_{\gamma\delta} G^{(0)}(\alpha,\gamma;E)$$
$$\times (-1) i^2 \tfrac{1}{2} \int \frac{dE_1}{2\pi} \int \frac{dE_2}{2\pi} \sum_{\lambda,\epsilon,\theta} \sum_{\zeta,\xi,\mu} \langle \gamma\lambda | V | \epsilon\theta \rangle$$
$$\times G^{(0)}(\epsilon,\zeta;E_1) G^{(0)}(\mu,\lambda;E_1+E_2-E)$$
$$\times G^{(0)}(\theta,\xi;E_2) \langle \zeta\xi | V | \delta\mu \rangle$$
$$\times G^{(0)}(\delta,\beta;E)$$

- Note structure of diagrams
- Noninteracting propagators at top and bottom (always)
- Include auxiliary potential

Rule 6 Label each U according to

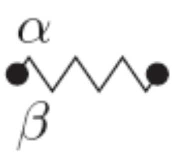

$$\Rightarrow \langle \alpha | U | \beta \rangle$$

Rule 7 Include a factor $(-1)^k$ and k additional propagators $G^{(0)}$

Organize diagrams

- Knowing how to calculate each term in the perturbation expansion of sp propagator is important but not sufficient
- Still requires to decide on appropriate approximations
- Approximations are always necessary
- Even if V "weak", not useful to do traditional perturbation theory
- Example: first-order term has double pole and does not correspond to Lehmann representation
- Reorganize expansion such that solutions (even if approximate) do!
- Requires infinite summations

- **Dyson equation ≈ Schrödinger-like equation for particles in the medium**

Diagrams so far (symmetrized)

- First-order

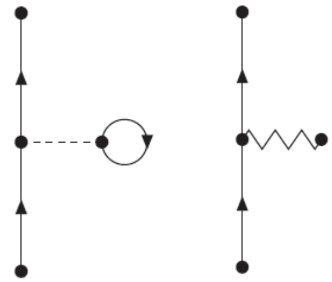

- Second order

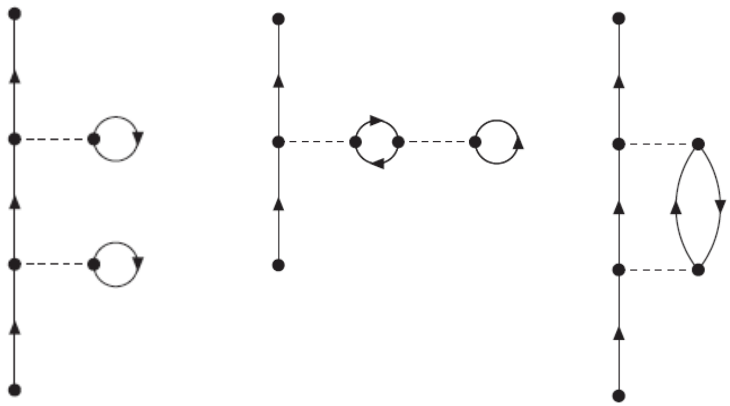

- Including U

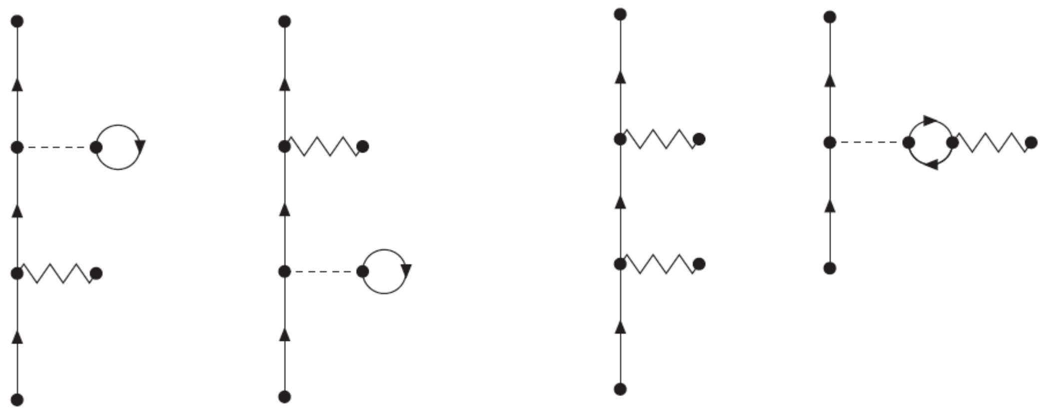

Summarize all orders

- Write sum of all diagrams

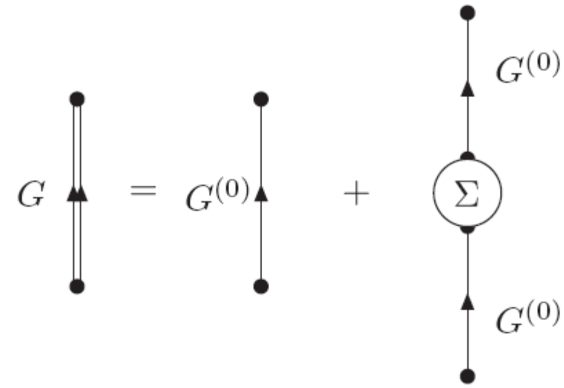

- Introducing the reducible self-energy --> sum all terms without top and bottom noninteracting propagators
- Remember

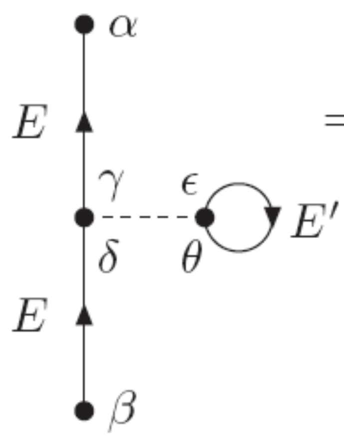

$$\Rightarrow \sum_{\gamma\delta} G^{(0)}(\alpha,\gamma;E)$$

$$\times \; -i\sum_{\epsilon\theta} \langle\gamma\epsilon|\, V \,|\delta\theta\rangle \int_{C\uparrow} \frac{dE'}{2\pi} G^{(0)}(\theta,\epsilon;E')$$

$$\times \; G^{(0)}(\delta,\beta;E)$$

- Lowest-order self-energy expression with V

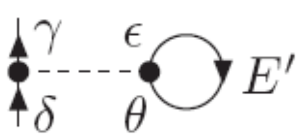

$$\Rightarrow \; -i\sum_{\epsilon\theta} \langle\gamma\epsilon|\, V \,|\delta\theta\rangle \int_{C\uparrow} \frac{dE'}{2\pi} G^{(0)}(\theta,\epsilon;E')$$

Second-order self-energy terms

- V only

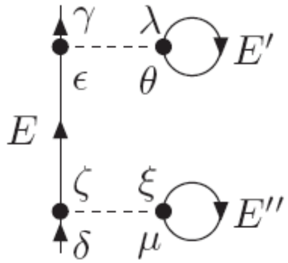

$$\Rightarrow\ (-1)^2 i^2 \sum_{\epsilon,\zeta}\sum_{\lambda,\theta}\int_{C\uparrow}\frac{dE'}{2\pi}\,\langle\gamma\lambda|\,V\,|\epsilon\theta\rangle\, G^{(0)}(\theta,\lambda;E')$$
$$\times\, G^{(0)}(\epsilon,\zeta;E)\sum_{\xi,\mu}\int_{C\uparrow}\frac{dE''}{2\pi}\,\langle\zeta\xi|\,V\,|\delta\mu\rangle\, G^{(0)}(\mu,\xi;E'')$$

$$\Rightarrow\ i^2\sum_{\epsilon\theta}\sum_{\lambda\zeta}\int_{C\uparrow}\frac{dE'}{2\pi}$$

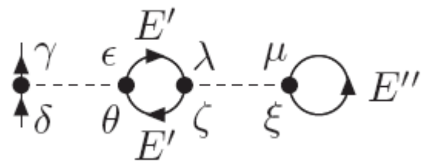

$$\times\ \langle\gamma\epsilon|\,V\,|\delta\theta\rangle\, G^{(0)}(\lambda,\epsilon;E')G^{(0)}(\theta,\zeta;E')$$
$$\times\ \sum_{\mu\xi}\int_{C\uparrow}\frac{dE''}{2\pi}\,\langle\zeta\xi|\,V\,|\lambda\mu\rangle\, G^{(0)}(\mu,\xi;E'')$$

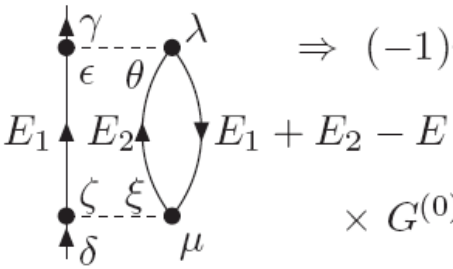

$$\Rightarrow\ (-1)i^2\frac{1}{2}\int\frac{dE_1}{2\pi}\int\frac{dE_2}{2\pi}\sum_{\lambda,\epsilon,\theta}\sum_{\zeta,\xi,\mu}\langle\gamma\lambda|\,V\,|\epsilon\theta\rangle$$
$$\times\ G^{(0)}(\epsilon,\zeta;E_1)G^{(0)}(\mu,\lambda;E_1+E_2-E)$$
$$\times\ G^{(0)}(\theta,\xi;E_2)\,\langle\zeta\xi|\,V\,|\delta\mu\rangle$$

- additional terms

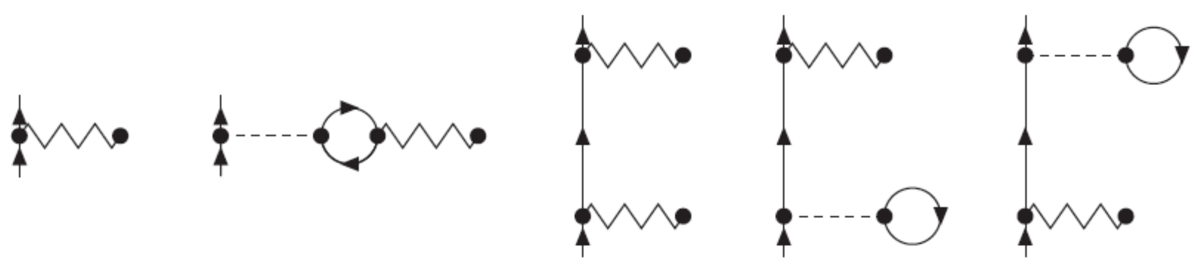

a) b) c) d) e)

Irreducible self-energy

- Consider only self-energy terms that cannot be separated into two pieces by cutting only one noninteracting sp propagator
- Irreducible self-energy Σ^*
- vs reducible self-energy Σ
- Expansion organized as

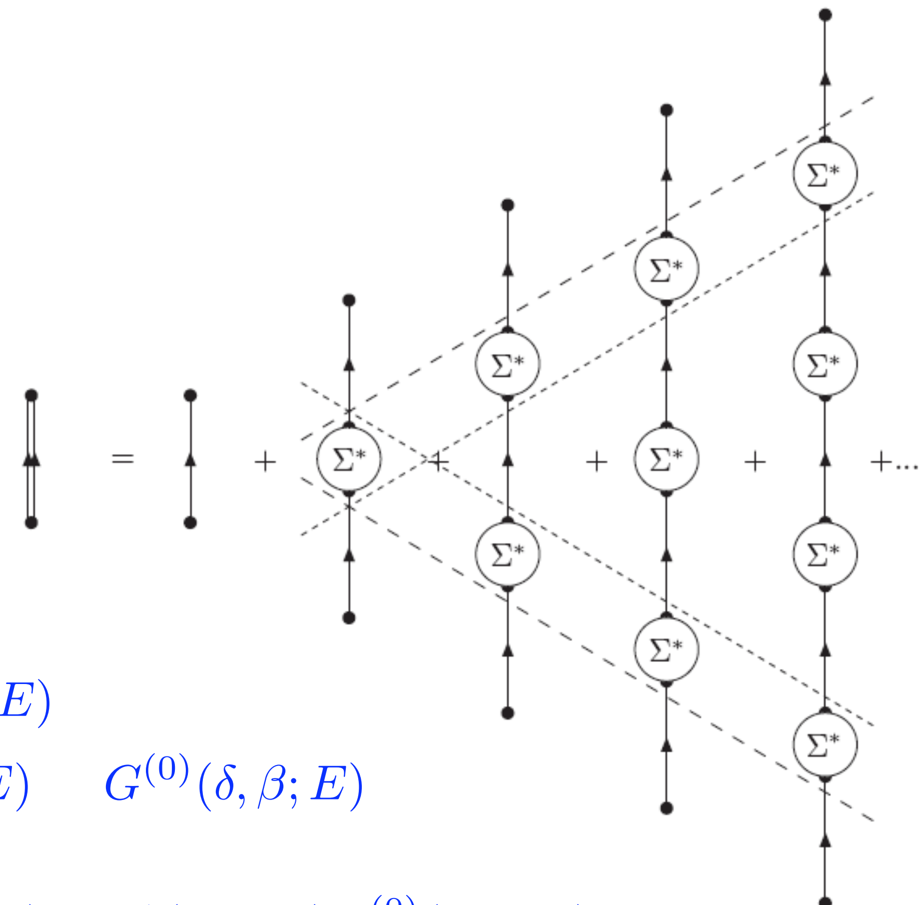

$$G(\alpha,\beta;E) = G^{(0)}(\alpha,\beta;E)$$

$$+\sum_{\gamma,\delta} G^{(0)}(\alpha,\gamma;E) \quad \Sigma^*(\gamma,\delta;E) \quad G^{(0)}(\delta,\beta;E)$$

$$+\sum_{\gamma,\delta,\epsilon,\theta} G^{(0)}(\alpha,\gamma;E)\Sigma^*(\gamma,\epsilon;E) \quad G^{(0)}(\epsilon,\theta;E) \quad \Sigma^*(\theta,\delta;E)G^{(0)}(\delta,\beta;E)$$

$$+ \quad \ldots..$$

Dyson equation

- Remember sp problem summations
- Same here: sum below short-dashed line (positive slope)

★ $$G(\alpha,\beta;E) = G^{(0)}(\alpha,\beta;E) + \sum_{\gamma,\delta} G^{(0)}(\alpha,\gamma;E)\Sigma^*(\gamma,\delta;E)G(\delta,\beta;E)$$

- Sum above short-dashed line (negative slope)

$$G(\alpha,\beta;E) = G^{(0)}(\alpha,\beta;E) + \sum_{\gamma,\delta} G(\alpha,\gamma;E)\Sigma^*(\gamma,\delta;E)G^{(0)}(\delta,\beta;E)$$

- As in sp problem yields eigenvalue problem or scattering equation
- Diagrammatically ★

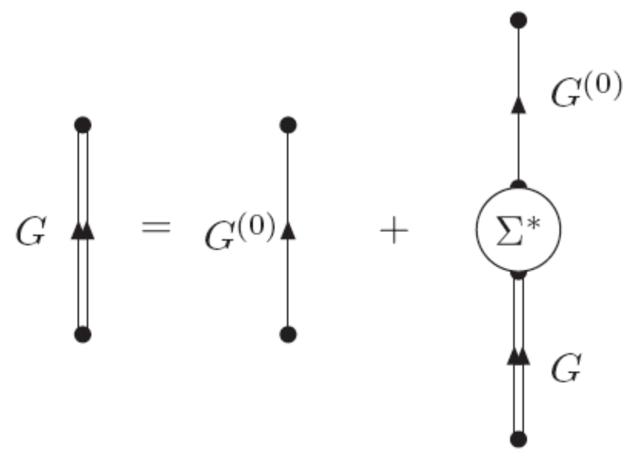

Reducible self-energy

- Similar organization defines scattering matrix for elastic scattering of projectile from target with identical particles!
- Sum terms between dashed lines

$$\Sigma(\gamma,\delta;E) = \Sigma^*(\gamma,\delta;E)$$
$$+\sum_{\epsilon,\theta}\Sigma^*(\gamma,\epsilon;E)\quad G^{(0)}(\epsilon,\theta;E)\quad \Sigma^*(\theta,\delta;E)$$
$$+\sum_{\epsilon,\theta,\zeta,\xi}\Sigma^*(\gamma,\epsilon;E)G^{(0)}(\epsilon,\theta;E)\quad \Sigma^*(\theta,\zeta;E)\quad G^{(0)}(\zeta,\xi;E)\Sigma^*(\xi,\delta;E)$$
$$+\quad .....$$

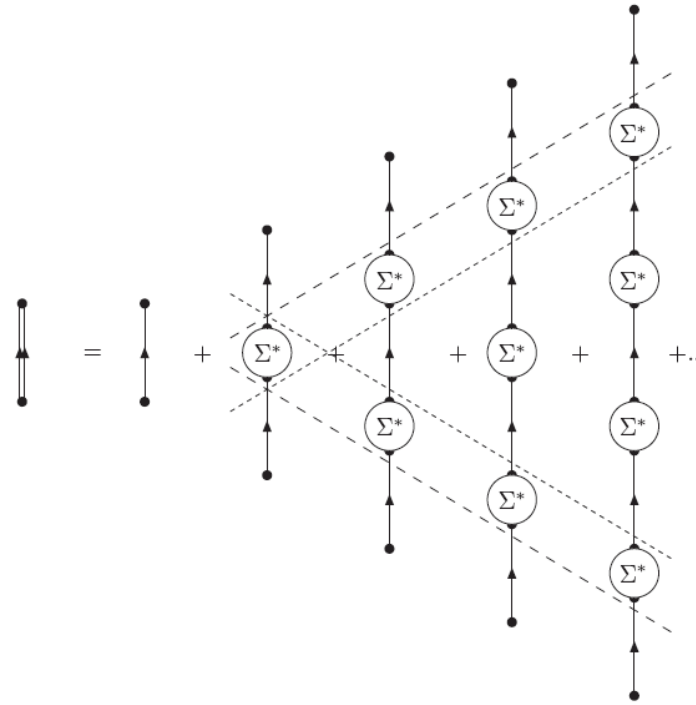

- Sum to all orders

$$\Sigma(\gamma,\delta;E) = \Sigma^*(\gamma,\delta;E) + \sum_{\epsilon,\theta}\Sigma^*(\gamma,\epsilon;E)G^{(0)}(\epsilon,\theta;E)\Sigma(\theta,\delta;E)$$

- or

$$\Sigma(\gamma,\delta;E) = \Sigma^*(\gamma,\delta;E) + \sum_{\epsilon,\theta}\Sigma(\gamma,\epsilon;E)G^{(0)}(\epsilon,\theta;E)\Sigma^*(\theta,\delta;E)$$

Direct knockout reactions

- Atoms: (e,2e) reaction
- Nuclei: (e,e'p) reaction [and others like (p,2p), (d,^{3}He), (p,d), etc.]
- Physics: transfer large amount of momentum and energy to a bound particle; detect ejected particle together with scattered projectile → construct spectral function
- Simple analysis
- Initial state: ground state $\left|\Psi_i\right\rangle = \left|\Psi_0^N\right\rangle$
- Final state: $\left|\Psi_f\right\rangle = a_{\boldsymbol{p}}^\dagger \left|\Psi_n^{N-1}\right\rangle$
- Probe: acts as one-body excitation operator transferring momentum $\hbar\boldsymbol{q}$ to a particle

$$\rho(\boldsymbol{q}) = \sum_{j=1}^{N} \exp\left(i\boldsymbol{q}\cdot\boldsymbol{r}_j\right)$$

- 2nd quantization (no spin) $\hat{\rho}(\boldsymbol{q}) = \sum_{\boldsymbol{p},\boldsymbol{p}'} \left\langle \boldsymbol{p}\right| \exp\left(i\boldsymbol{q}\cdot\boldsymbol{r}\right) \left|\boldsymbol{p}'\right\rangle a_{\boldsymbol{p}}^\dagger a_{\boldsymbol{p}'} = \sum_{\boldsymbol{p}} a_{\boldsymbol{p}}^\dagger a_{\boldsymbol{p}-\hbar\boldsymbol{q}}$

Transition matrix element

- Impulse approximation: struck particle is ejected

$$\begin{aligned}\langle \Psi_f |\, \hat{\rho}(\boldsymbol{q})\, | \Psi_i \rangle &= \sum_{\boldsymbol{p}'} \langle \Psi_n^{N-1} |\, a_{\boldsymbol{p}} a^\dagger_{\boldsymbol{p}'} a_{\boldsymbol{p}'-\hbar\boldsymbol{q}}\, | \Psi_0^N \rangle \\ &= \sum_{\boldsymbol{p}'} \langle \Psi_n^{N-1} |\, \delta_{\boldsymbol{p}',\boldsymbol{p}} a_{\boldsymbol{p}'-\hbar\boldsymbol{q}} + a^\dagger_{\boldsymbol{p}'} a_{\boldsymbol{p}'-\hbar\boldsymbol{q}} a_{\boldsymbol{p}}\, | \Psi_0^N \rangle \\ &\approx \langle \Psi_n^{N-1} |\, a_{\boldsymbol{p}-\hbar\boldsymbol{q}}\, | \Psi_0^N \rangle\end{aligned}$$

- Other assumption: final state ~ plane wave on top of N-1 particle eigenstate (more serious in practical experiments) but good approximation if ejectile momentum large enough
- Write $H_N = \sum_{i=1}^{N} \frac{\boldsymbol{p}_i^2}{2m} + \sum_{i<j=1}^{N} V(i,j) = H_{N-1} + \frac{\boldsymbol{p}_N^2}{2m} + \sum_{i=1}^{N-1} V(i,N)$
- last term FSI: interaction between ejected particle and others
- If relative momentum large enough, interaction can be neglected:
- PWIA = plane wave impulse approximation

Cross section

- Fermi's Golden Rule $d\sigma \sim \sum_n \delta(\hbar\omega + E_i - E_f) | \langle \Psi_f | \hat{\rho}(\boldsymbol{q}) | \Psi_i \rangle |^2$

- with energy transfer $\hbar\omega$ linking initial $E_i = E_0^N$
  and final state energy $E_f = E_n^{N-1} + \boldsymbol{p}^2/2m$

- Define $\boldsymbol{p}_{miss} = \boldsymbol{p} - \hbar\boldsymbol{q}$

$$E_{miss} = \boldsymbol{p}^2/2m - \hbar\omega = E_0^N - E_n^{N-1}$$

- Rewrite knockout cross section

$$\begin{aligned} d\sigma &\sim \sum_n \delta(E_{miss} - E_0^N + E_n^{N-1}) | \langle \Psi_n^{N-1} | a_{\boldsymbol{p}_{miss}} | \Psi_0^N \rangle |^2 \\ &= S_h(\boldsymbol{p}_{miss}; E_{miss}) \end{aligned}$$

- More comprehensive treatment requires inclusion of FSI

(e,2e) data for atoms

- Start with Hydrogen
- Ground state wave function $\phi_{1s}(\boldsymbol{p}) = \frac{2^{3/2}}{\pi} \frac{1}{(1+p^2)^2}$
- (e,2e) removal amplitude

$$\langle 0| a_{\boldsymbol{p}} |n=1,\ell=0\rangle = \langle \boldsymbol{p} |n=1,\ell=0\rangle = \phi_{1s}(\boldsymbol{p})$$

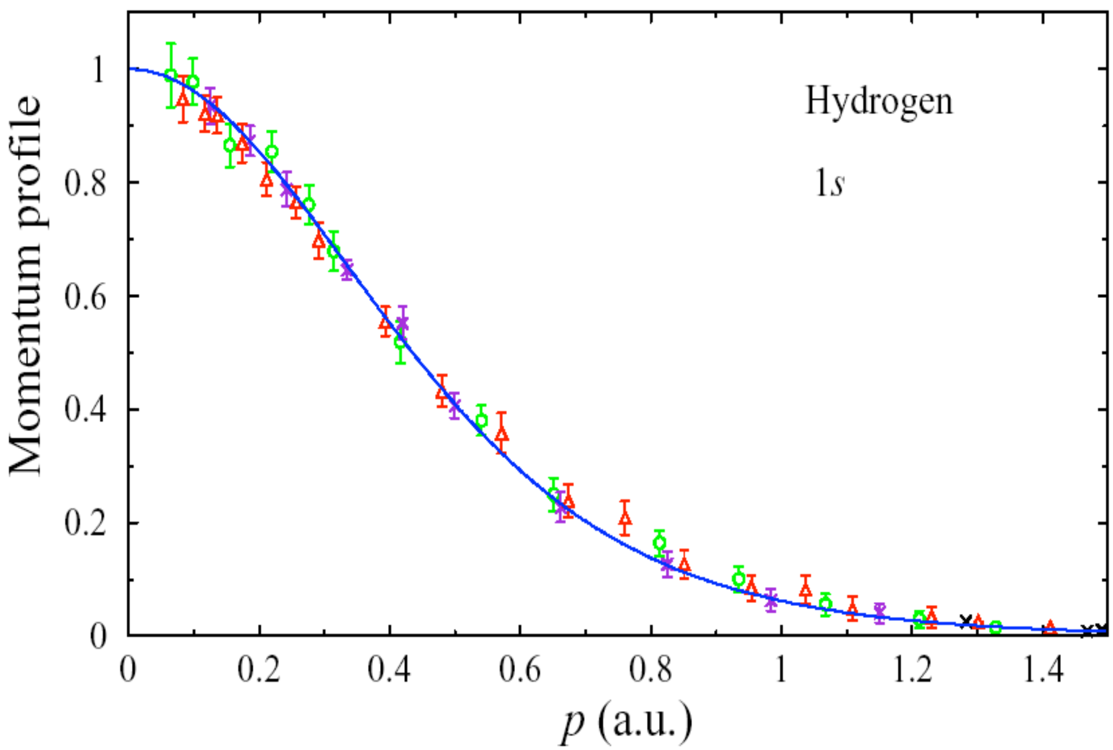

Hydrogen 1s wave function "seen" experimentally
Phys. Lett. 86A, 139 (1981)

(e,e'p) data for nuclei

- Requires DWIA
- Distorted waves required to describe elastic proton scattering at the energy of the ejected proton
- Consistent description requires that cross section at different energy for the outgoing proton is changed accordingly
- Requires substantial beam energy and momentum transfer
- Initiated at Saclay and perfected at NIKHEF, Amsterdam
- Also done at Mainz and currently at Jefferson Lab
- Momentum dependence of cross section dominated by the corresponding sp wave function of the nucleon before it is removed

Momentum profiles for nucleon removal

- Closed-shell nuclei
- NIKHEF data, L. Lapikás, Nucl. Phys. A553, 297c (1993)

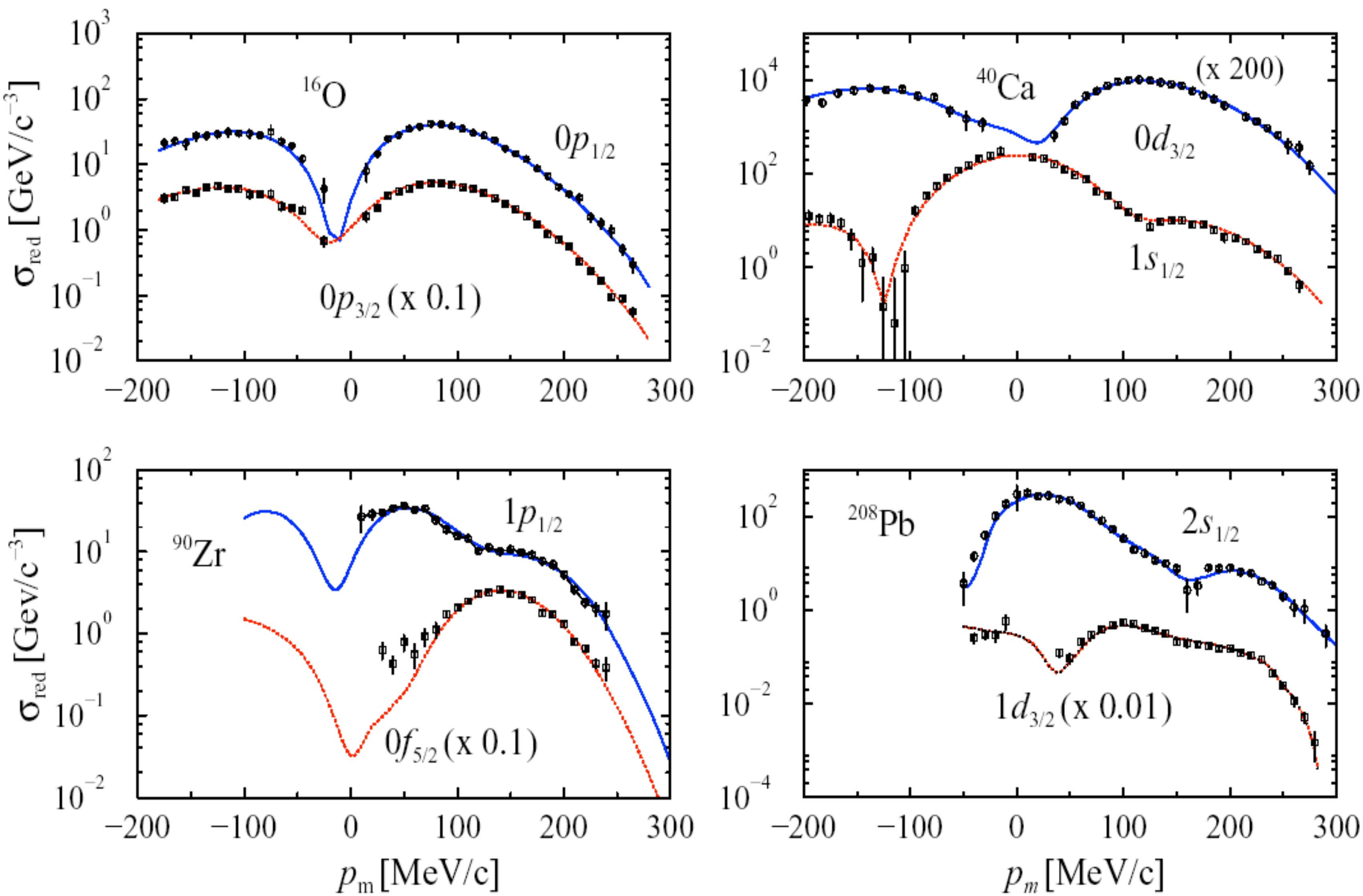

But...

- Spectroscopic factors substantially smaller than simple IPM

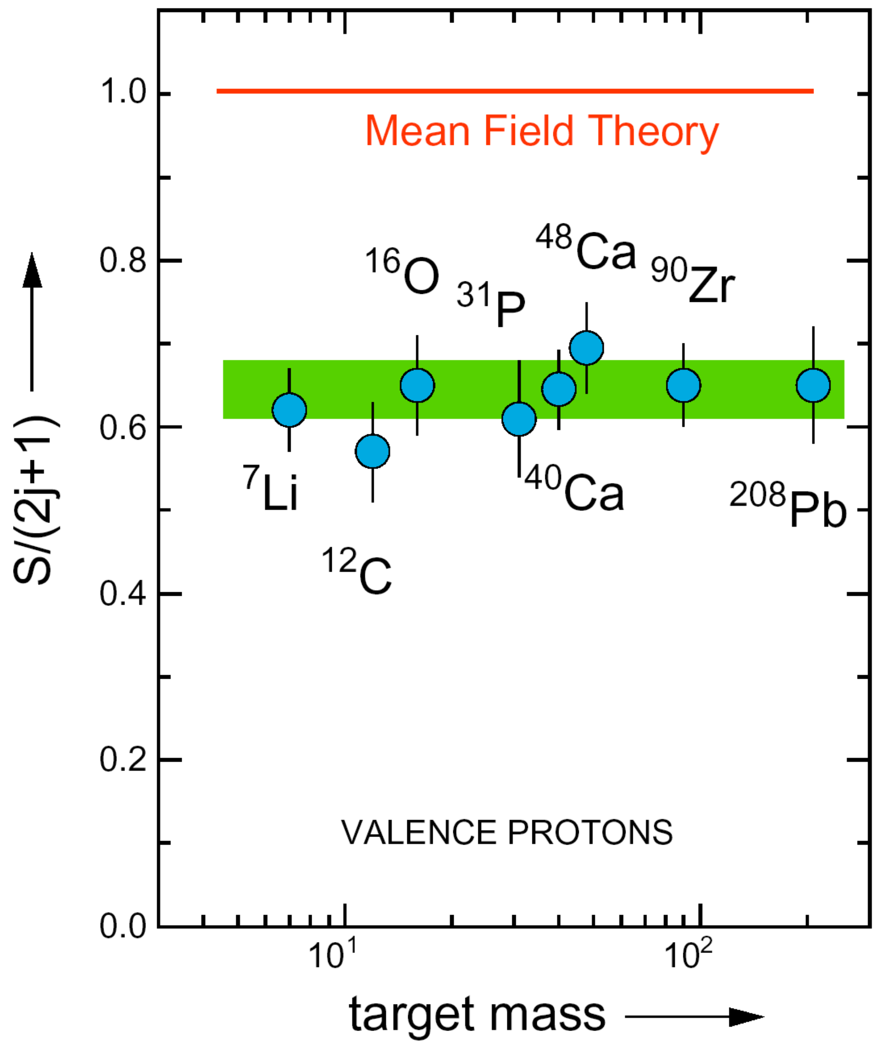

Remember

- ^{208}Pb sp levels

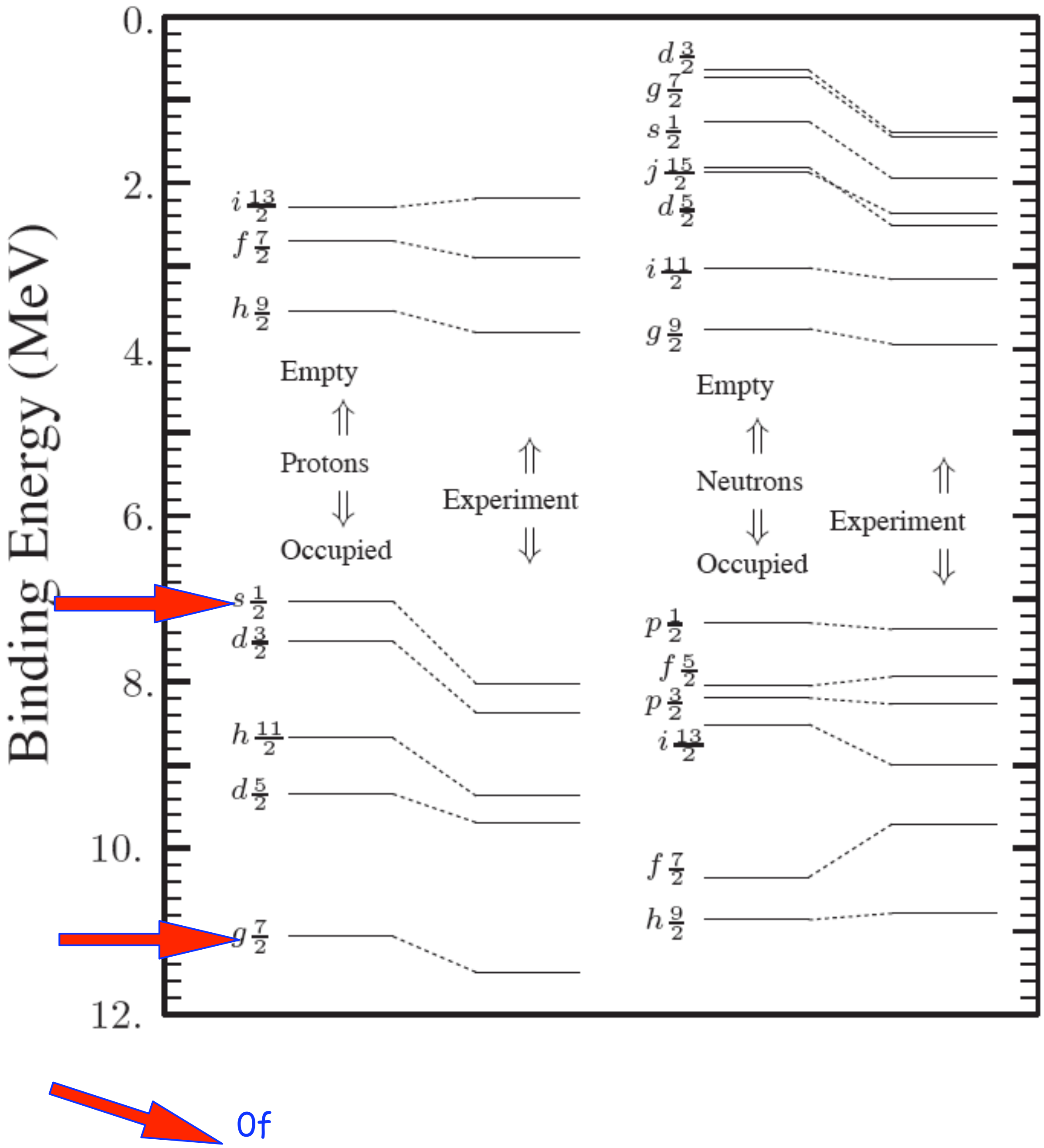

Fragmentation patterns

- ^{208}Pb(e,e'p) NIKHEF data: Quint thesis
- $S(2s_{1/2})=0.65$
- other data:
- $n(2s_{1/2})=0.75$

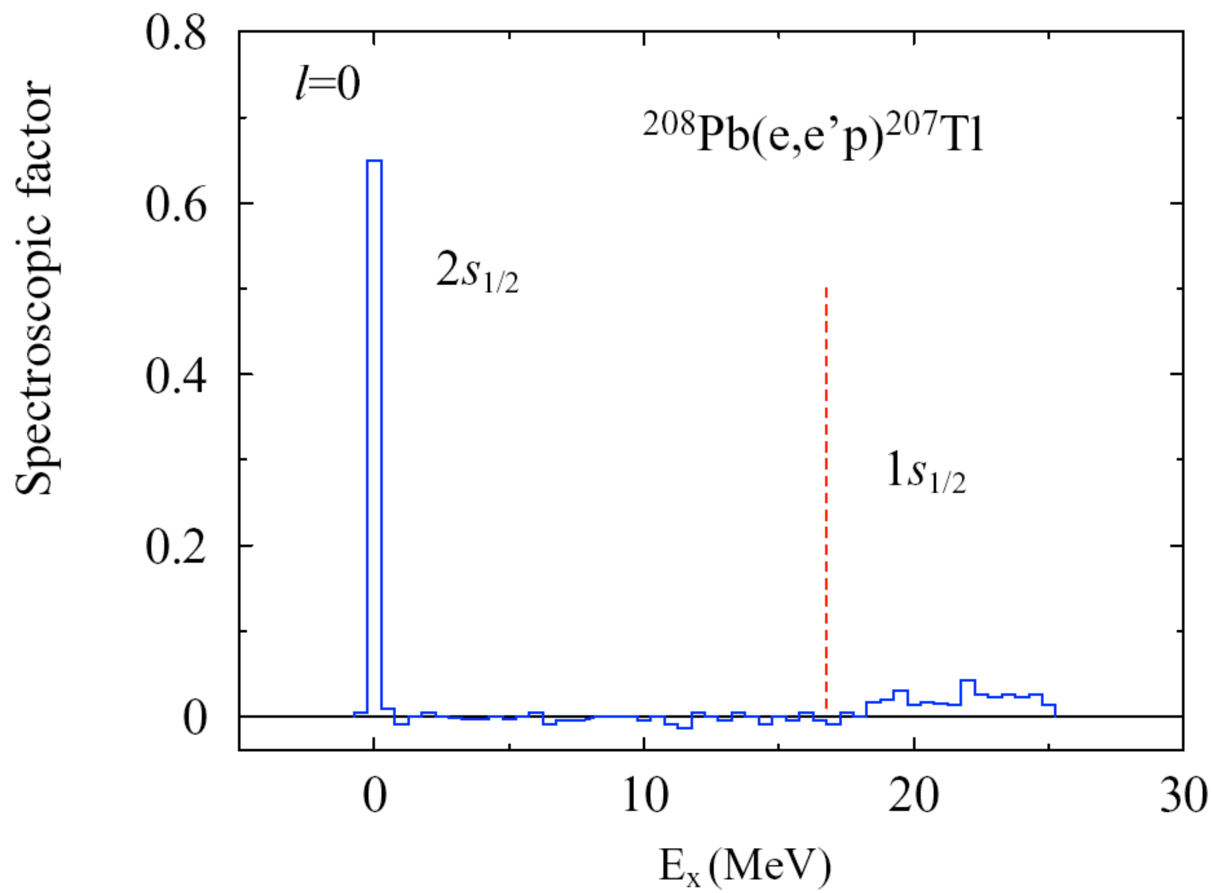

- very different from atoms

Fragmentation patterns

- ^{208}Pb(e,e'p) NIKHEF data: Quint NIKHEF thesis (1988)

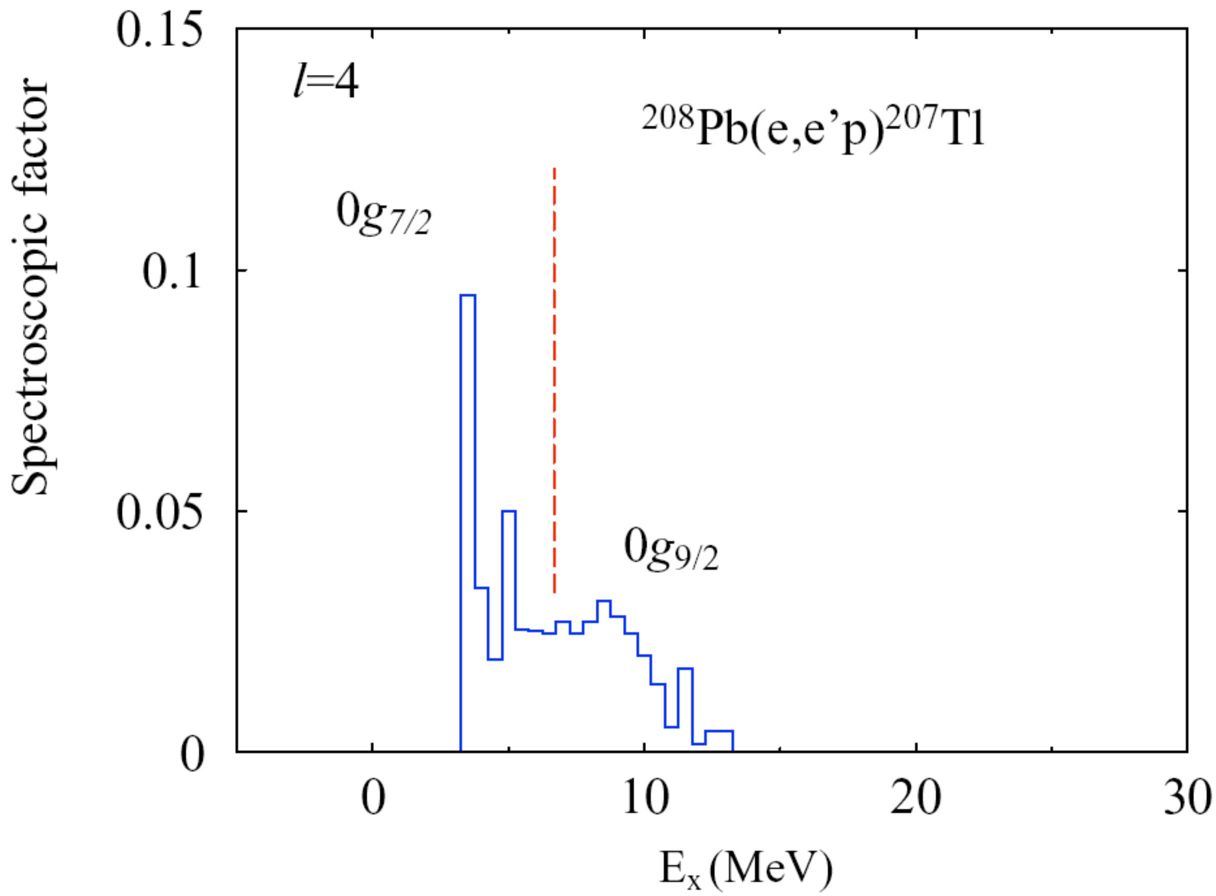

- start of strong fragmentation
- also very different from atoms

Fragmentation patterns

- ^{208}Pb(e,e'p) NIKHEF data: Quint thesis

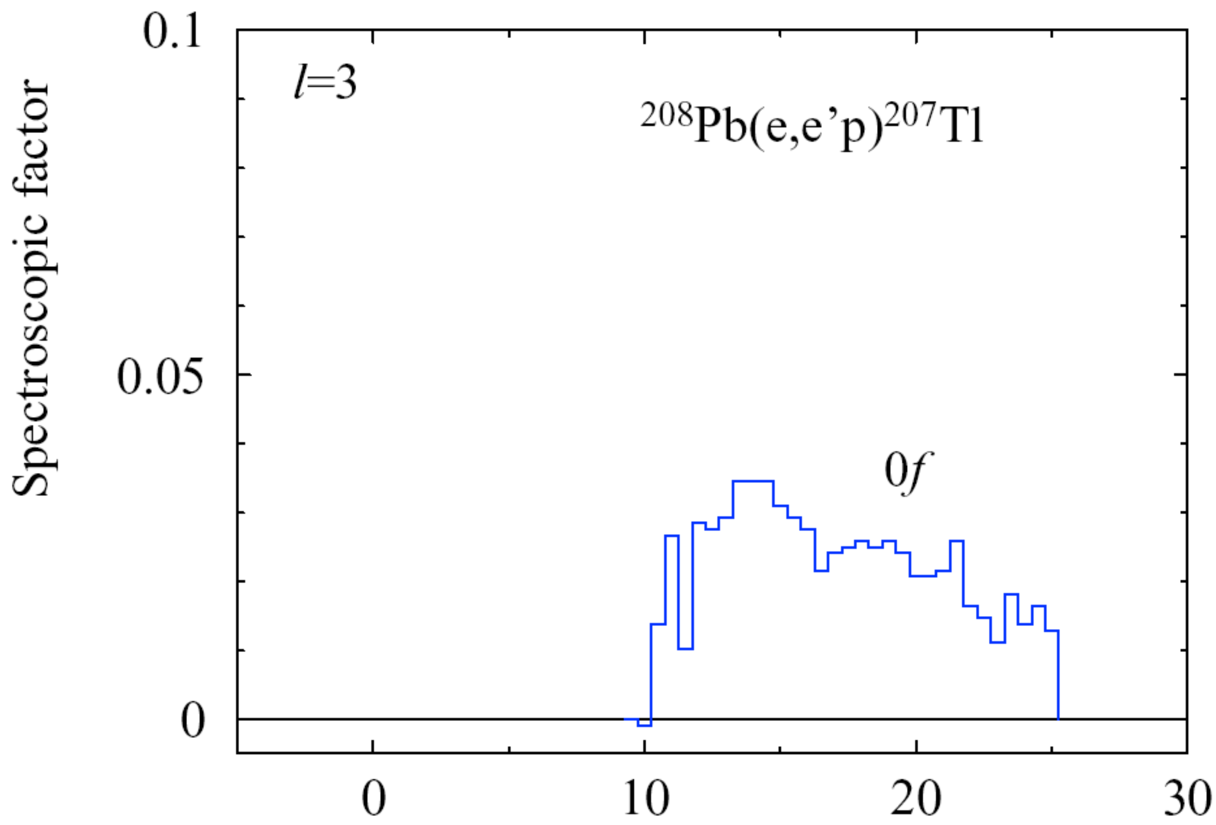

- deeply bound states: strong fragmentation
- again different from atoms

^{16}O data from Saclay

- Simple interpretation!
- Mougey et al., Nucl. Phys. A335, 35 (1980)

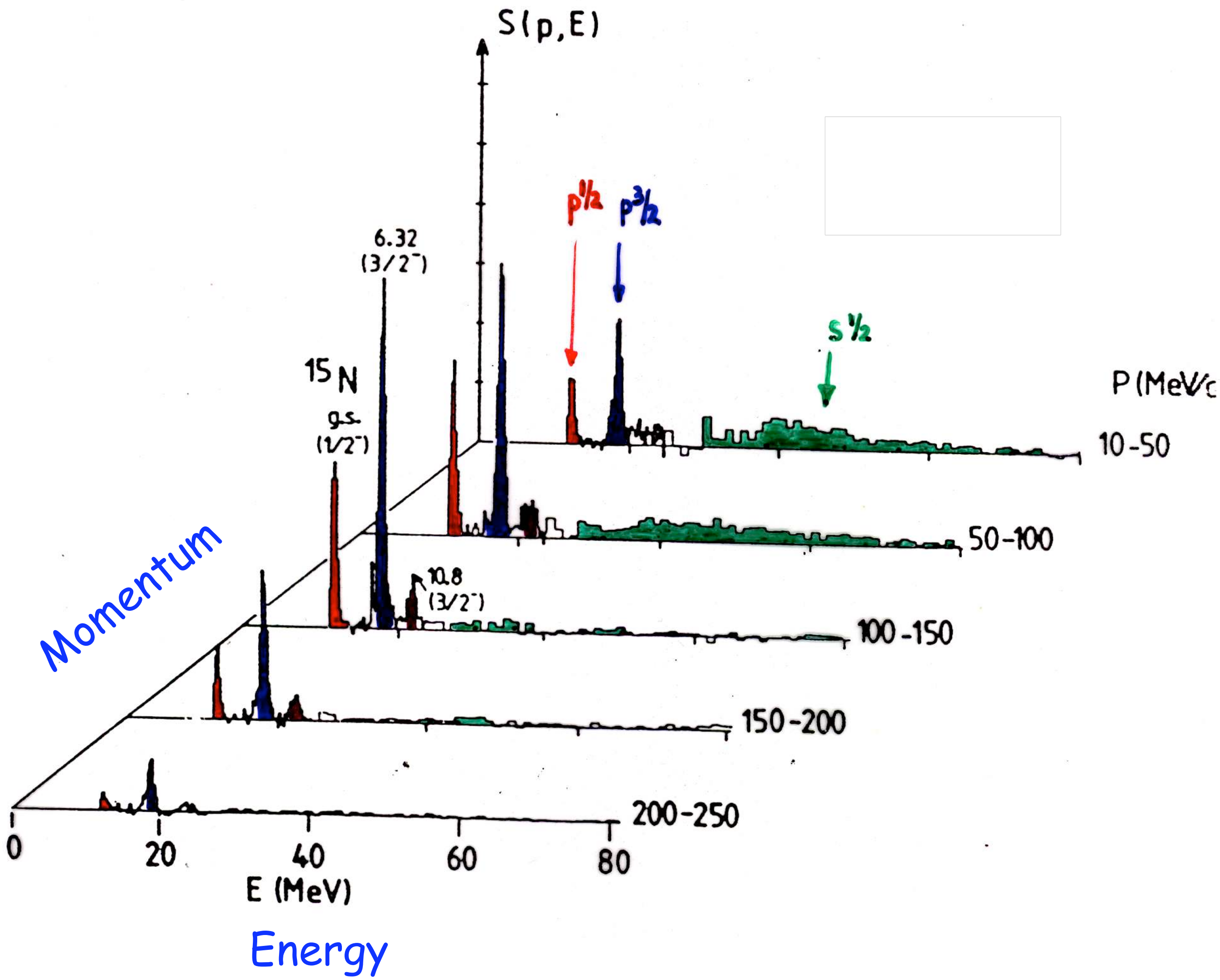

Pb experiment at NIKHEF (as yet unpublished)

- 100 MeV missing energy
- 270 MeV/c missing momentum
- complete IPM domain

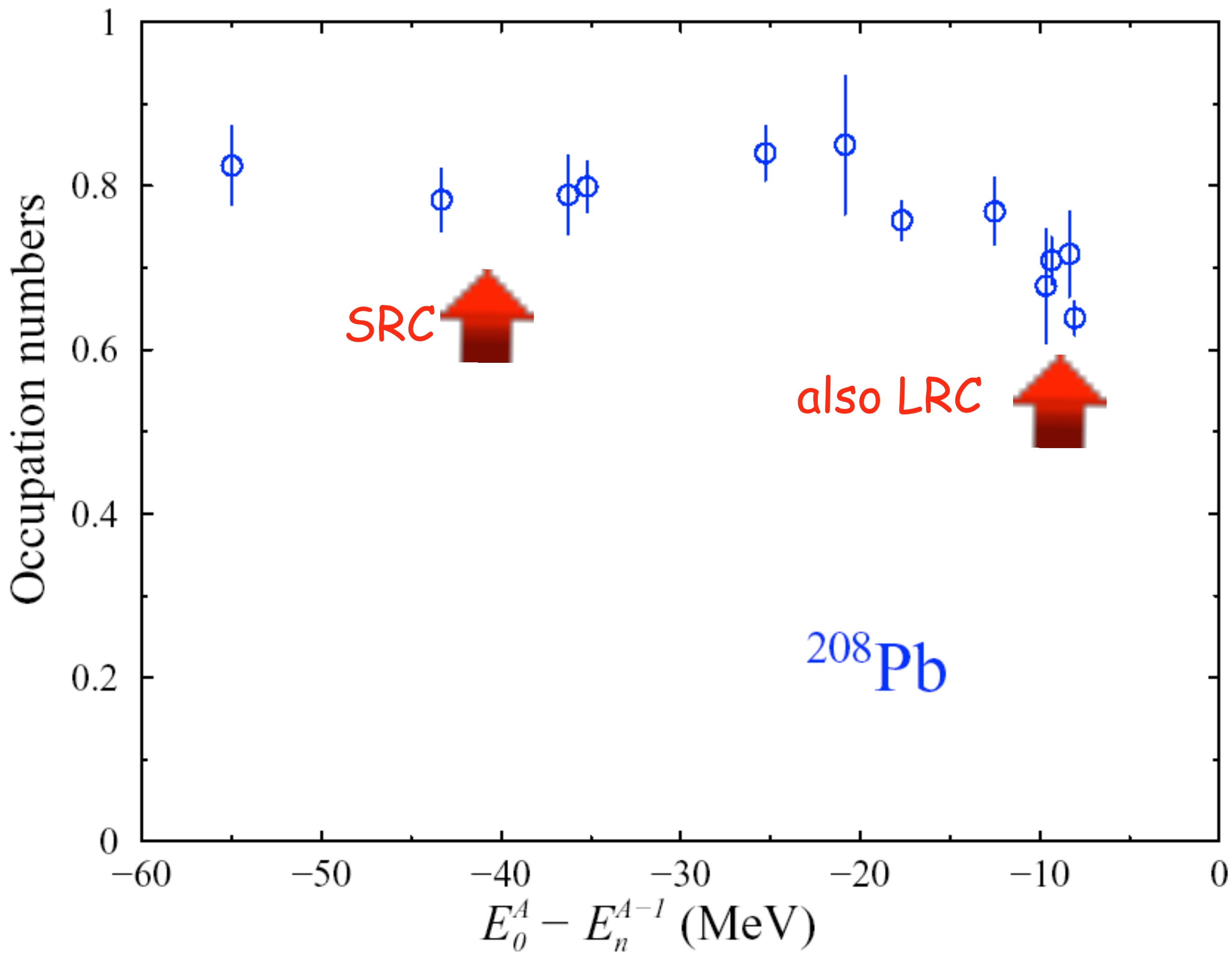

Interpretation of (e,e′p)

- Can spectroscopic factors be measured?
  - Short answer: yes, at low temperature in quantum fluids —> specific heat
  - Short answer: no, but…there are a lot consistency checks with other data
  - Note difference between spectroscopic factor and occupation
- Reaction model tested
  - Different proton energies —> same reduction factor
  - Coupled-channel calculation —> cross section identical for sp-like transitions
  - Meson-exchange currents —> no influence in parallel kinematics
  - Relativistic analysis —> same momentum profile!
    - But different spectroscopic factors!
    - Why?
  - Optical potential?
    - Local
    - Nondispersive

Deep-inelastic neutron scattering off quantum liquids

Liquid ^{3}He

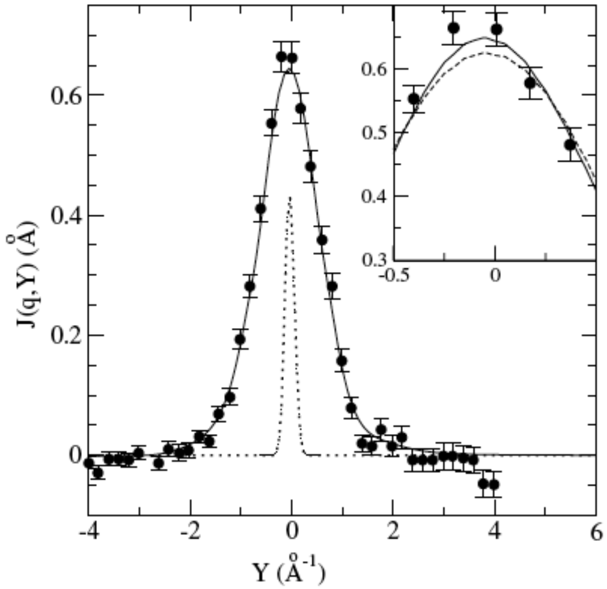

Response at 19.4 Å^{-1}

Probe: neutrons

R.T. Azuah et al., J. Low Temp. Phys. **101**, 951 (1995)

Theory: Monte Carlo n(k) & FSE (ρ_2) beyond IA

F. Mazzanti et al., Phys. Rev. Lett. **92**, 085301 (2004)

$$J(Y) = \frac{1}{2\pi^2 \rho} \int_{|Y|}^{\infty} dk\, k\, n(k)$$ IA result

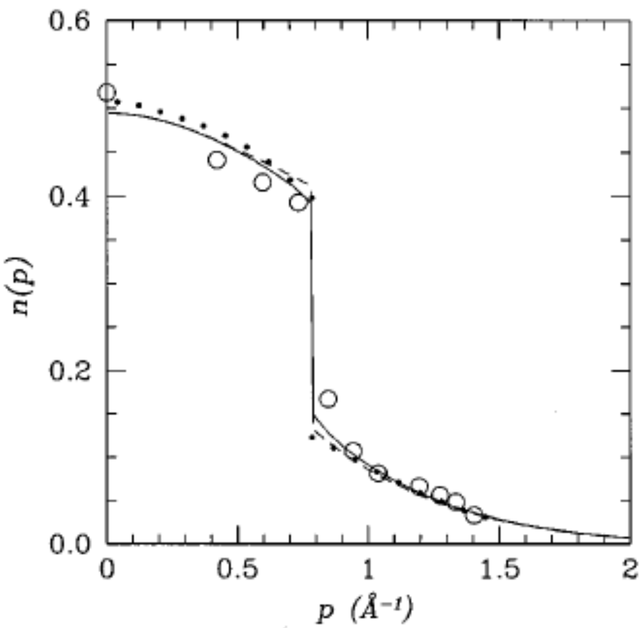

$$Y = \frac{m\omega}{q} - \frac{q}{2}$$ scaling variable

Momentum distribution liquid ^{3}He

S. Moroni et al., Phys. Rev. B**55**, 1040 (1997)

Comparison of DMC, GFMC, and VMC & HNC

Other experiments

- Difficulty of describing single-particle level structure
- Elastic electron scattering
  - Charge density
- Parity violating electron scattering
  - Weak charge density
- Elastic nucleon scattering
  - Usually done with fits using local "optical potentials" —> distorted waves
  - Link with single-particle propagator!
- Inelastic electron scattering to high-spin states

Phenomenological potential and experiment

- Now how to explain this potential …

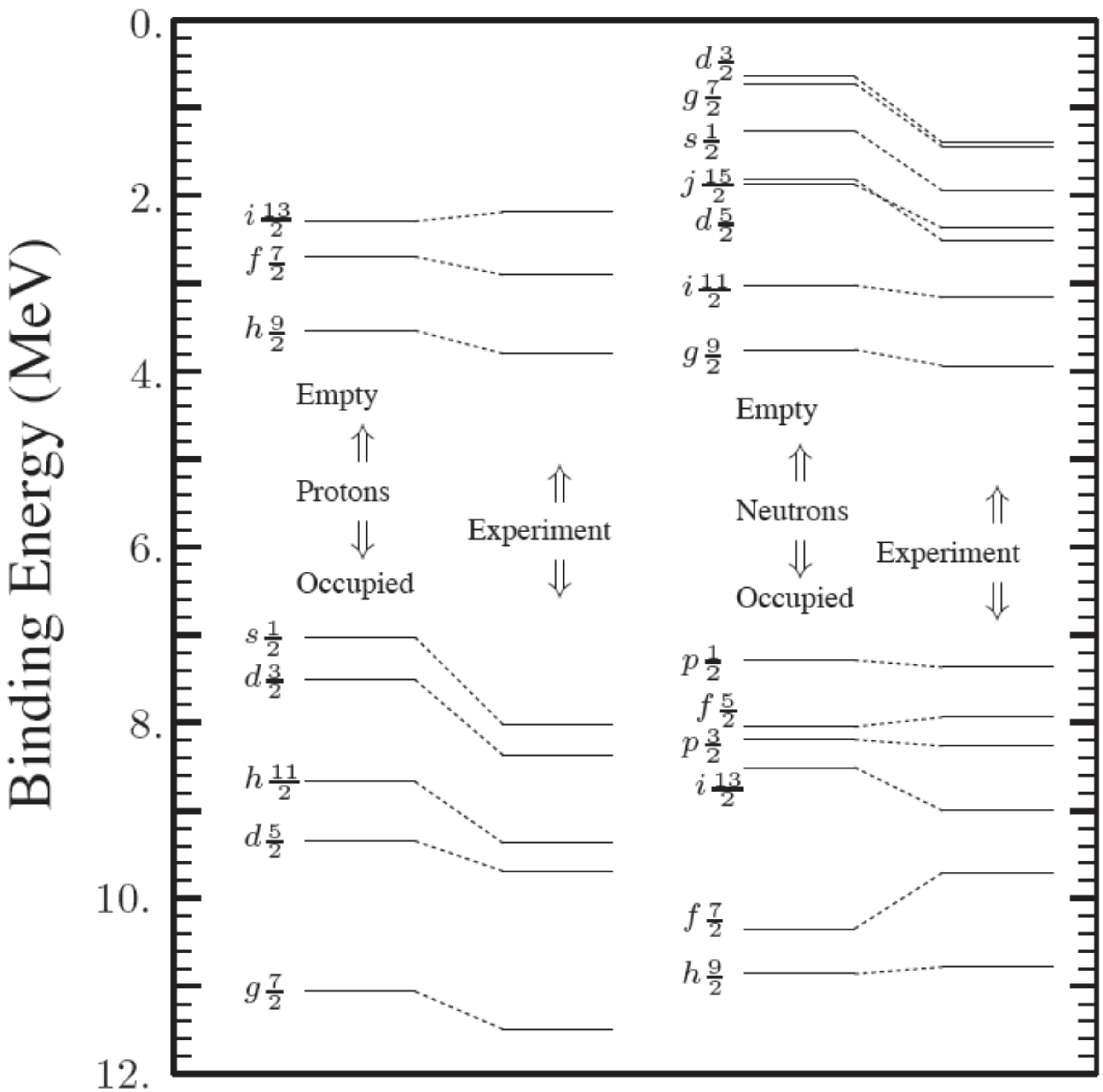

Typical mean-field calculation

- ph-gap too large
- Mahaux:
  - potential depends on energy
  - use dispersion relation
  - mean field is not sufficient

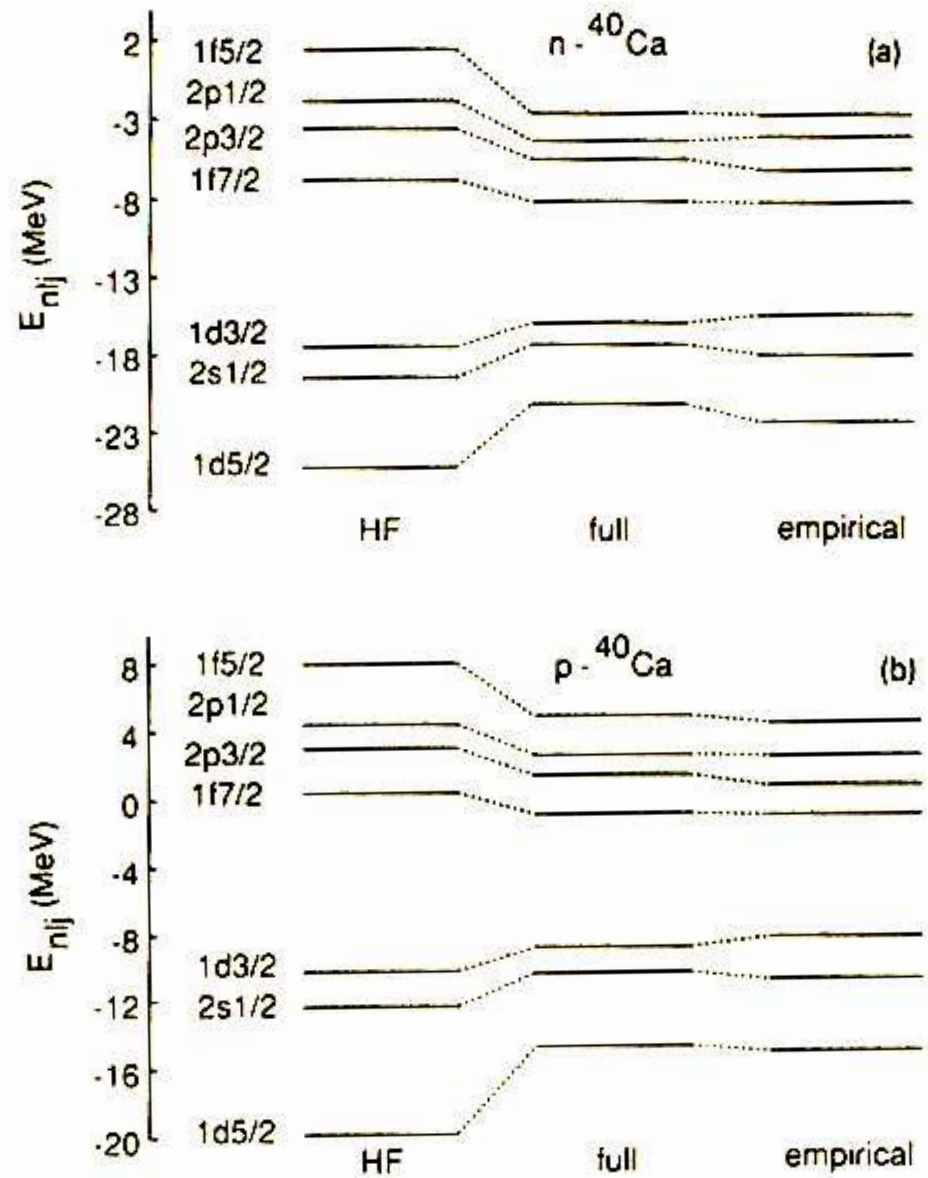

Nuclear charge density

- Mean field insufficient

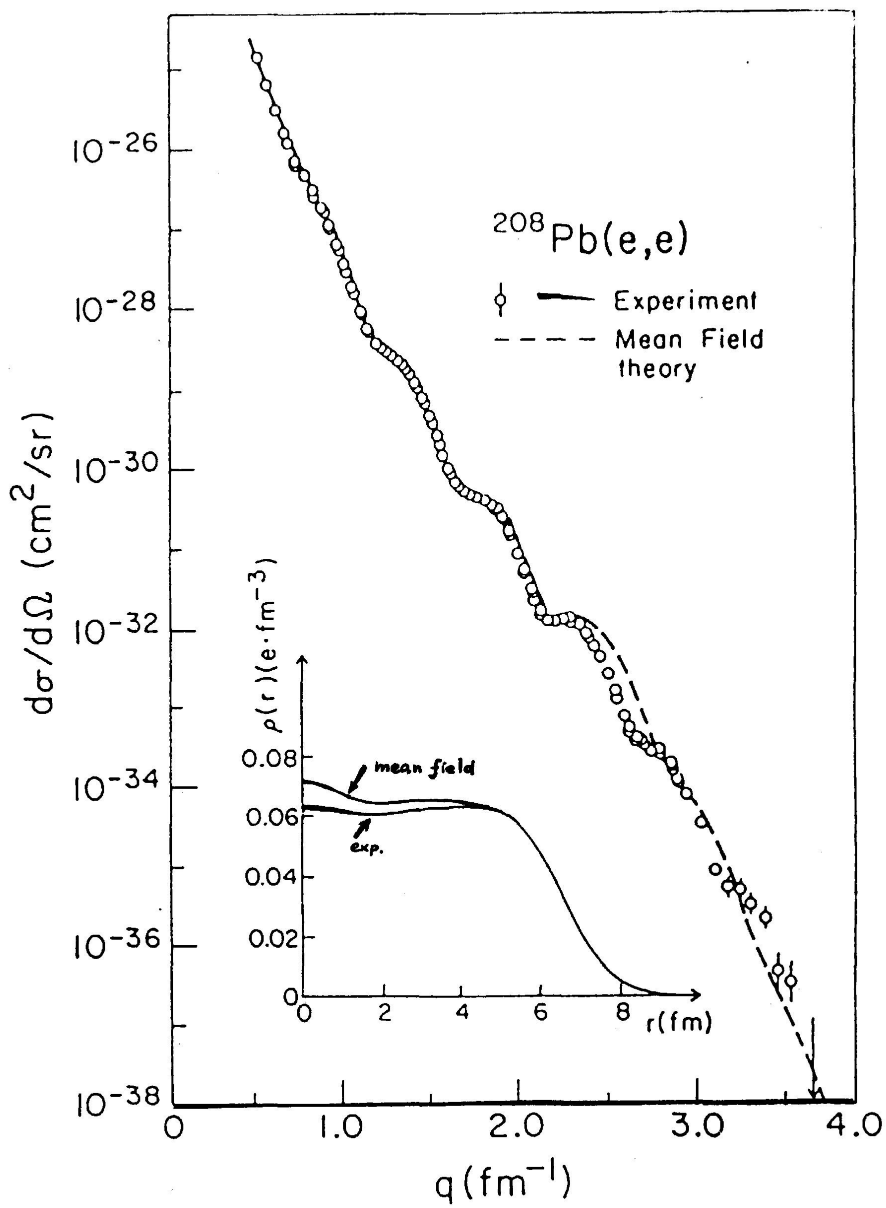

Parity violating electron scattering

- 3 Slides from Chuck Horowitz

Parity Violation Isolates Neutrons

- In Standard Model Z^0 boson couples to the weak charge.
- Proton weak charge is small:

$$Q_W^p = 1 - 4\sin^2\Theta_W \approx 0.05$$

- Neutron weak charge is big:

$$Q_W^n = -1$$

- Weak interactions, at low Q^2, probe neutrons.
- Parity violating asymmetry A_{pv} is cross section difference for positive and negative helicity electrons

$$A_{pv} = \frac{d\sigma/d\Omega_+ - d\sigma/d\Omega_-}{d\sigma/d\Omega_+ + d\sigma/d\Omega_-}$$

- A_{pv} from interference of photon and Z^0 exchange. In Born approximation

$$A_{pv} = \frac{G_F Q^2}{2\pi\alpha\sqrt{2}} \frac{F_W(Q^2)}{F_{\rm ch}(Q^2)}$$

$$F_W(Q^2) = \int d^3r \frac{\sin(Qr)}{Qr} \rho_W(r)$$

- Model independently map out distribution of weak charge in a nucleus.
- **Electroweak reaction free from most strong interaction uncertainties.**
  - Donnelly, Dubach, Sick first suggested PV to measure neutrons.

Result and plans

- At Jefferson Laboratory, 1.05 GeV electrons elastically scattered from thick ^{208}Pb foil. PRL **108**, 112502, PRC **85**, 032501
- A_{PV}=0.66 ±0.06(stat) ±0.014(sym) ppm
- Neutron skin thickness: R_n-R_p=$0.33^{+0.16}_{-0.18}$ fm
- Experiment achieved systematic error goals.
- Future plans: **PREX-II** (approved 25 days) Run ^{208}Pb again to accumulate more statistics. Goal: R_n to ±0.06 fm.
- **CREX**: Approved follow on for ^{48}Ca with goal: R_n to ±0.02 fm.

^{208}Pb results

PREX Results

- 1.05 GeV electrons elastically scattering at ~5 deg. from ^{208}Pb
- **A_{PV} = 0.657 ± 0.060(stat) ± 0.014(sys) ppm**
- The stat. error was not Paul (he is not so good at counting). The very small systematic error is Paul. He is very good at not counting in an extremely unbiased way.
- Paul has measured the weak form factor of ^{208}Pb. This is Fourier transform of weak charge density (divided by the large coherent weak charge) $F_W(q)$ = 0.204 ± 0.028 at q=.45 fm^{-1}
- Radius of weak charge distr. R_W = 5.83 ± 0.18 ± 0.03(model) fm

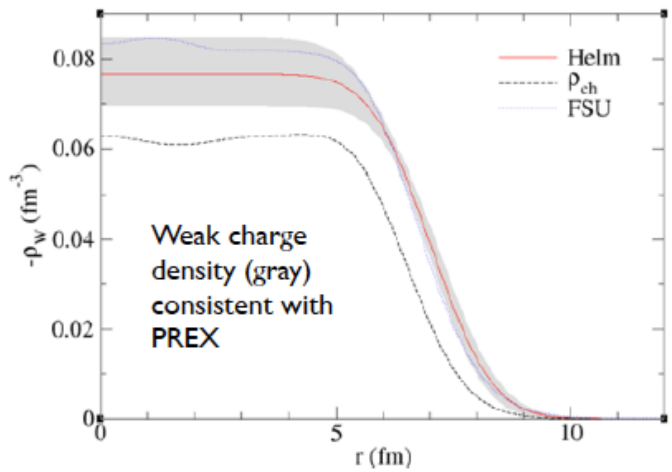

- Compare to charge radius R_{ch}=5.503 fm --> weak skin: $R_W - R_{ch}$ = 0.32 ± 0.18 ± 0.03 fm
- First observation that weak charge density more extended than (E+M) charge density --> weak skin.
- Unfold nucleon ff--> neutron skin: $R_n - R_p = 0.33^{+0.16}_{-0.18}$ fm

Where neutrons go for N>Z is very hot topic in nuclear physics

Elastic nucleon scattering

- Scattering from potential $\langle k_0|\mathcal{S}^\ell(E)|k_0\rangle = \left[1 - 2\pi i\left(\frac{mk_0}{\hbar^2}\right)\langle k_0|\mathcal{T}^\ell(E)|k_0\rangle\right] \equiv e^{2i\delta_\ell}$
- Potential real —> phase shift real
- Scattering amplitude

$$\begin{aligned} f(\theta,\phi) &= \sum_l \frac{2l+1}{k_0}\left\{\frac{-mk_0\pi}{\hbar^2}\right\}\langle k_0|\mathcal{T}^\ell(E)|k_0\rangle P_\ell(\cos\theta) \\ &= \sum_\ell \frac{2\ell+1}{k_0} e^{i\delta_\ell}\sin\delta_\ell P_\ell(\cos\theta) \end{aligned}$$

- Elastic nucleon scattering
  - Involves reducible self-energy (see also later)

$$\langle k_0|\,\mathcal{S}_{\ell j}(E)\,|k_0\rangle \equiv e^{2i\delta_{\ell j}} = 1 - 2\pi i\left(\frac{mk_0}{\hbar^2}\right)\langle k_0|\,\Sigma_{\ell j}(E)\,|k_0\rangle$$

  - Scattering amplitude

$$f_{m_s',m_s}(\theta,\phi) = -\frac{4m\pi^2}{\hbar^2}\langle \boldsymbol{k}'m_s'|\Sigma(E)|\boldsymbol{k}m_s\rangle$$

  - Phase shift now includes imaginary part when potential is absorptive

Spin-orbit physics included

- Scattering amplitude $f_{m_s',m_s}(\theta,\phi) = -\frac{4m\pi^2}{\hbar^2}\langle \boldsymbol{k}' m_s' | \Sigma(E) | \boldsymbol{k} m_s \rangle$
- Rewrite $[f(\theta,\phi)] = \mathcal{F}(\theta) I + \boldsymbol{\sigma}\cdot\hat{\boldsymbol{n}}\mathcal{G}(\theta)$
  - with
$$\hat{\boldsymbol{n}} = \frac{\boldsymbol{k}\times\boldsymbol{k}'}{|\boldsymbol{k}\times\boldsymbol{k}'|} = \frac{\hat{\boldsymbol{k}}\times\hat{\boldsymbol{k}}'}{\sin\theta}$$
  - then
$$\mathcal{F}(\theta) = \frac{1}{2ik}\sum_{\ell=0}^{\infty}\left[(\ell+1)\left\{e^{2i\delta_{\ell+}}-1\right\} + \ell\left\{e^{2i\delta_{\ell-}}-1\right\}\right] P_\ell(\cos\theta)$$
$$\mathcal{G}(\theta) = \frac{\sin\theta}{2k}\sum_{\ell=1}^{\infty}\left[e^{2i\delta_{\ell+}} - e^{2i\delta_{\ell-}}\right] P_\ell'(\cos\theta)$$
  - Unpolarized differential cross section $\left(\frac{d\sigma}{d\Omega}\right)_{unpol} = |\mathcal{F}|^2 + |\mathcal{G}|^2$

Cross sections

- Total elastic cross section

$$\sigma_{tot}^{el} = \frac{\pi}{k^2} \sum_{\ell=0}^{\infty} \frac{\left|(\ell+1)\left\{e^{2i\delta_{\ell+}}-1\right\}+\ell\left\{e^{2i\delta_{\ell-}}-1\right\}\right|^2}{2\ell+1} + \frac{\pi}{k^2} \sum_{\ell=0}^{\infty} \frac{\ell(\ell+1)\left|e^{2i\delta_{\ell+}}-e^{2i\delta_{\ell-}}\right|^2}{2\ell+1}$$

- Reaction cross section (only when there is absorption)

$$\sigma_{tot}^{r} = \sum_{\ell=0}^{\infty} \frac{\pi}{k^2} \left[(2\ell+1)-(\ell+1)\left|e^{2i\delta_{\ell+}}\right|^2-\ell\left|e^{2i\delta_{\ell-}}\right|^2\right]$$

- Total cross section $\sigma_T = \sigma_{tot}^{el} + \sigma_{tot}^{r}$
- Polarization and spin rotation

$$P(\theta) = \frac{2\mathrm{Re}\{\mathcal{F}(\theta)\mathcal{G}^*(\theta)\}}{|\mathcal{F}|^2+|\mathcal{G}|^2} \qquad Q(\theta) = \frac{2\mathrm{Im}\{\mathcal{F}(\theta)\mathcal{G}^*(\theta)\}}{|\mathcal{F}|^2+|\mathcal{G}|^2}$$

Fit and predictions of n & p elastic scattering cross sections

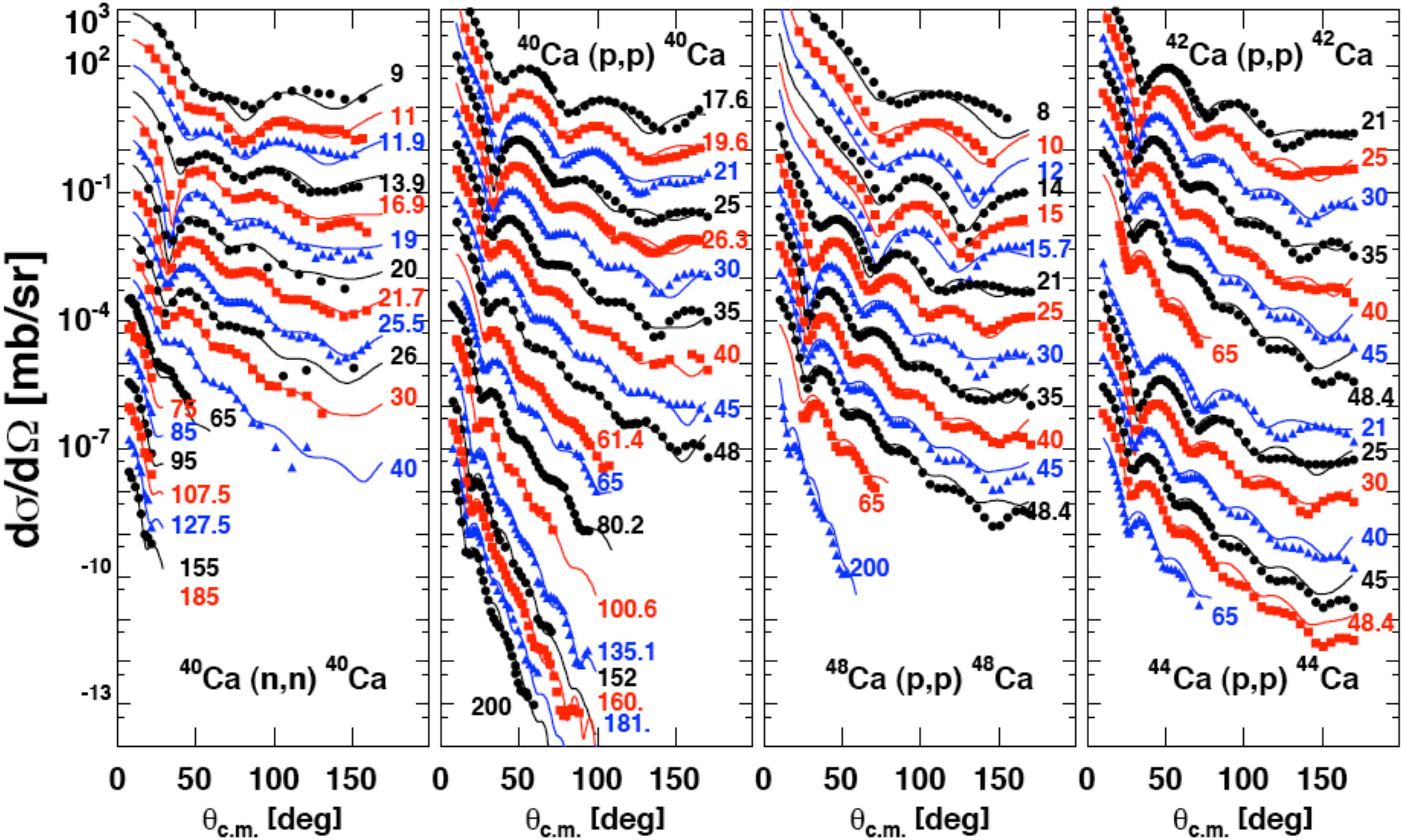

Present fit and predictions of polarization data

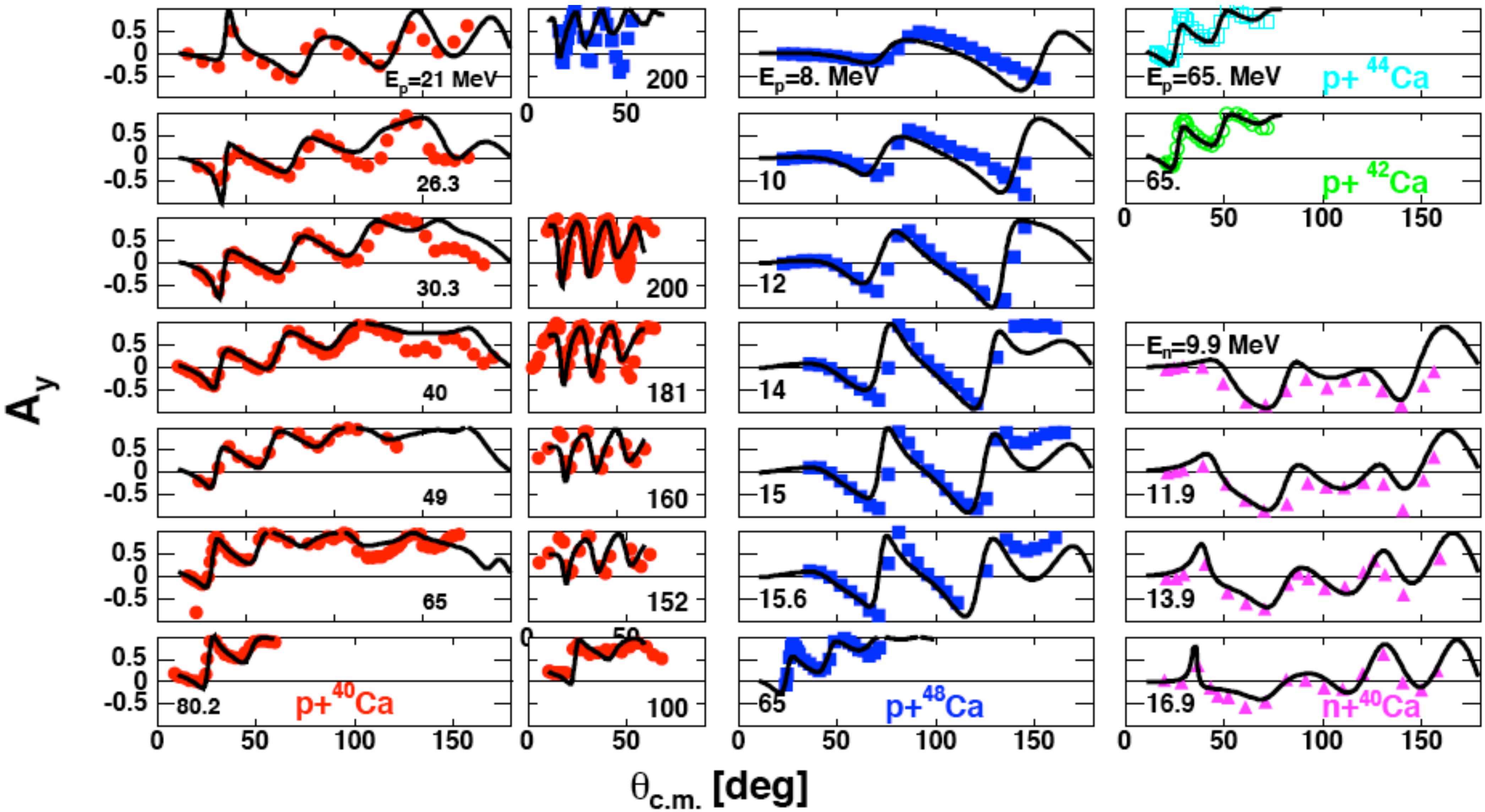

Nucleon correlations

Reaction cross section ^{40}Ca and ^{48}Ca

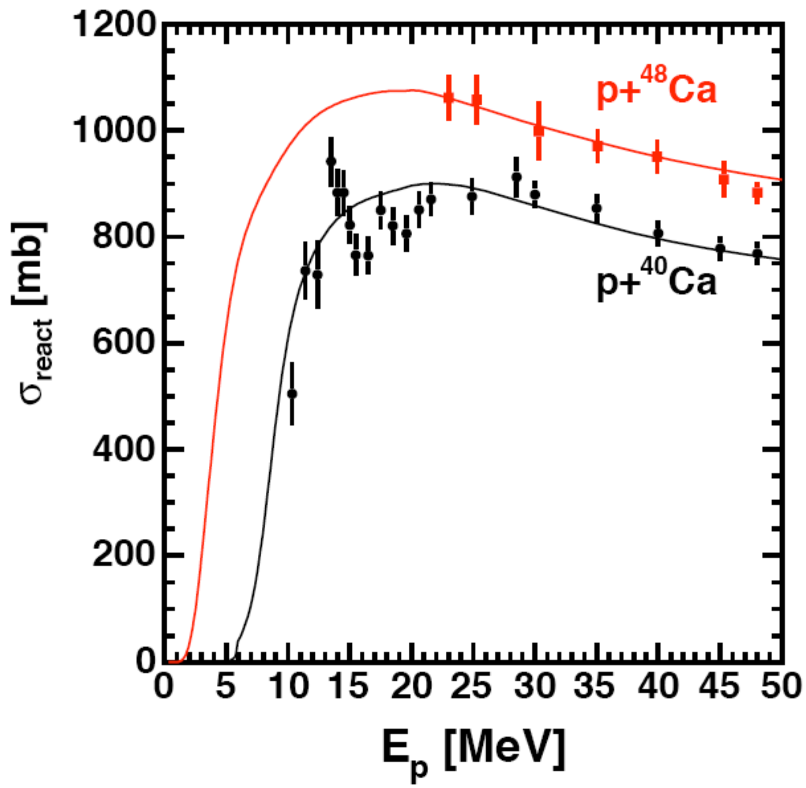

Loss of flux in the elastic channel

More absorption of protons
in ^{48}Ca than ^{40}Ca below 50 MeV

Inelastic electron scattering

- Older but important data:

PHYSICAL REVIEW C VOLUME 20, NUMBER 2 AUGUST 1979

High-spin states of $J^{\pi} = 12^-, 14^-$ in ^{208}Pb studied by (e, e')

J. Lichtenstadt, J. Heisenberg,* C. N. Papanicolas, and C. P. Sargent
Bates Linear Accelerator Center and Massachusetts Institute of Technology, Cambridge, Massachusetts 02139

A. N. Courtemanche and J. S. McCarthy
University of Virginia, Charlottesville, Virginia 22901

(Received 2 March 1979)

TABLE I. High-spin ($J > 9$), single p-h transitions in ^{208}Pb, whose single p-h energies are below 8 MeV.

Transition		E_{sph} (MeV)	Magnetic					Electric				
Neutron (p-h)												
$2g_{9/2}$	$i_{13/2}$	5.06			11^+		9^+				10^+	
$j_{15/2}$	$2f_{5/2}$	5.42					9^+				10^+	
$j_{15/2}$	$3p_{3/2}$	5.66					9^+					
$i_{11/2}$	$i_{13/2}$	5.84			11^+		9^+		12^+		10^+	
$j_{15/2}$	$i_{13/2}$	6.48	14^-	12^-		10^-		13^-		11^-		9^-
$i_{11/2}$	$2f_{7/2}$	6.55										9^-
$3d_{5/2}$	$i_{13/2}$	6.63					9^+					
$2g_{9/2}$	$h_{9/2}$	6.84										9^-
$j_{15/2}$	$2f_{7/2}$	7.19			11^+		9^+				10^+	
$2g_{7/2}$	$i_{13/2}$	7.55					9^+				10^+	
$i_{11/2}$	$h_{9/2}$	7.62				10^-						9^-
Proton (p-h)												
$h_{9/2}$	$h_{11/2}$	5.65					9^+				10^+	
$2f_{7/2}$	$h_{11/2}$	6.54					9^+					
$i_{13/2}$	$h_{11/2}$	7.26		12^-		10^-				11^-		9^-
$i_{13/2}$	$2d_{5/2}$	7.59					9^+					

High-spin states are simple ph configurations…

- But cross section reduced by a factor of about 2

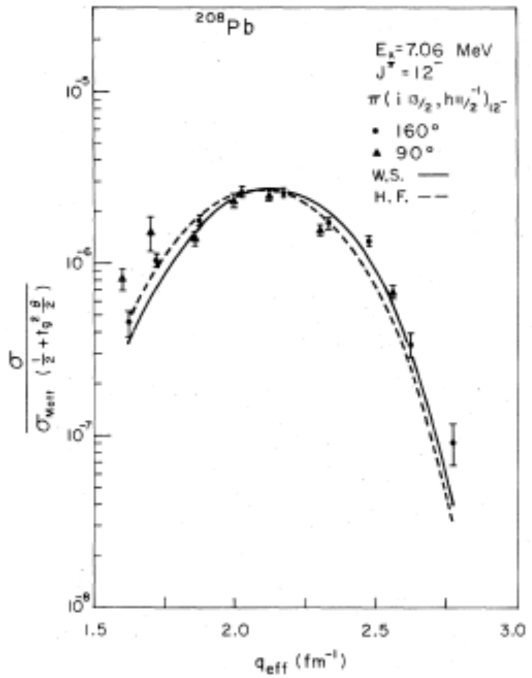

FIG. 3. Cross section of the level at 7.06 MeV with $J^\pi=12^-$. The dashed and solid lines are single p-h predictions of the $\pi(i_{13/2}h_{11/2}^{-1})_{12^-}$ transition, using Hartree-Fock and Woods-Saxon wave functions, respectively. The curves presented are the "reduced cross sections" calculated in DWBA at 160°. The calculation at 90° is almost identical to that at 160°, to the accuracy of the graph.

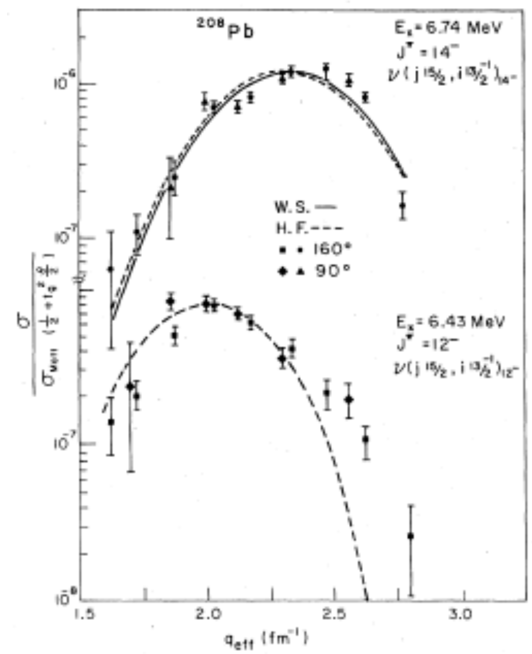

FIG. 4. Cross sections of the levels at 6.74 and 6.43 MeV, with $J^\pi=14^-$, 12^-, respectively. The dashed and solid lines are single p-h predictions of the $\nu(j_{15/2}i_{13/2}^{-1})_{14^-,12^-}$ transitions, using Hartree-Fock and Woods-Saxon wave functions, respectively. For calculational details see text.

The overall strength observed when fitted either with HF wave functions or with the Woods-Saxon wave functions comes out to be only $(50\pm3.5)\%$ of the predicted single particle strength for the $\nu(j_{15/2}, i_{13/2})_{14^-,12^-}$, as well as for the $\pi(i_{13/2}, h_{11/2}^{-1})_{12^-}$ configuration. This quenching is about the same as that observed in the $M9$ moment of the ground state of ^{209}Bi, coming from the odd $h_{9/2}$ proton.[16]

Analyzed in 1984

- Experimental quenching factors

VOLUME 53, NUMBER 12 PHYSICAL REVIEW LETTERS 17 SEPTEMBER 1984

Occupation Probabilities of Shell-Model Orbits in the Lead Region

V. R. Pandharipande, C. N. Papanicolas, and J. Wambach
Department of Physics, University of Illinois at Urbana-Champaign, Urbana, Illinois 61801
(Received 7 May 1984)

TABLE I. The energy, E, and spin and parity, J^π, of the final state are given in the first two columns. The next three columns give the shell-model description of the transition. The last two columns give the experimental value of Q, the quenching factor, and the reference.

E (MeV)	J^π	h	p	t	Q	Ref.
			^{208}Pb(e,e')			
4.04	7^-	$2f_{5/2}$	$2g_{9/2}$	N	0.51 ± 0.05	5
6.10	12^+	$1i_{13/2}$	$1i_{11/2}$	N	0.65 ± 0.04	6
6.43	12^-	$1i_{13/2}$	$1j_{15/2}$	N	0.71 ± 0.05	7
6.74	14^-	$1i_{13/2}$	$1j_{15/2}$	N	0.71 ± 0.05	7
7.06	12^-	$1h_{11/2}$	$1i_{13/2}$	P	0.71 ± 0.05	7
			^{207}Pb(e,e')			
0.57	$\frac{5}{2}^-$	$2f_{5/2}$	$3p_{1/2}$	N	0.65 ± 0.05	8
0.90	$\frac{3}{2}^-$	$3p_{3/2}$	$3p_{1/2}$	N	0.65 ± 0.05	8
1.63	$\frac{13}{2}^+$	$1i_{13/2}$	$3p_{1/2}$	N	0.47 ± 0.05	8
2.34	$\frac{7}{2}^-$	$2f_{7/2}$	$3p_{1/2}$	N	0.55 ± 0.05	8
2.73	$\frac{9}{2}^+$	$3p_{1/2}$	$2g_{9/2}$	N	0.50 ± 0.05	8
3.51	$\frac{11}{2}^+$	$3p_{1/2}$	$1i_{11/2}$	N	0.65 ± 0.05	8

More recent results

PHYSICAL REVIEW C VOLUME 45, NUMBER 6 JUNE 1992

High resolution electron scattering from high spin states in ^{208}Pb

J. P. Connelly,* D. J. DeAngelis, J. H. Heisenberg, F. W. Hersman, W. Kim, M. Leuschner, T. E. Milliman, and J. Wise†
Department of Physics, University of New Hampshire, Durham, New Hampshire 03824

C. N. Papanicolas
Department of Physics and Nuclear Physics Laboratory, University of Illinois, 1110 West Green Street, Urbana, Illinois 61801
(Received 2 March 1992)

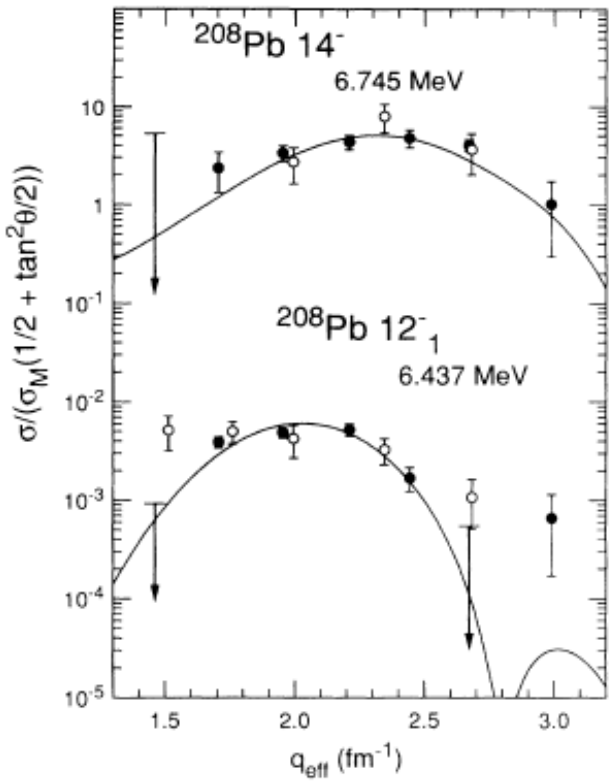

FIG. 4. $M14$ (6.745 MeV) and $M12$ (6.347 MeV) form factors with DWBA Woods-Saxon fits. The 6.745 MeV form factor is scaled by 1000. Forward angle data are represented by the open data points; the 155° data are presented by the solid data points.

TABLE I. High spin transitions seen in this experiment with the dominant 1p-1h configuration and the normalization factor (N_q) of the Woods-Saxon DWBA fits to the data. An asterisk indicates the assignment of J^π is from this experiment.

Energy (MeV)	J^π	1p-1h configuration	N_q
5.010	9^+	$\nu(2g_{9/2},1i^{-1}_{13/2})$	0.54±0.01
5.260	9^{+*}	$\pi(1h_{9/2},1h^{-1}_{11/2})$	0.53±0.04
5.291	11^{+*}	$\nu(2g_{9/2},1i^{-1}_{13/2})$	0.38±0.03
5.860	11^{+*}	$\nu(1i_{11/2},1i^{-1}_{13/2})$	0.61±0.05
5.954	9^{+*}	$\nu(1i_{11/2},1i^{-1}_{13/2})$	0.50±0.05
		$\pi(2f_{7/2},1h^{-1}_{11/2})$	0.19±0.03
6.110	12^+	$\nu(1i_{11/2},1i^{-1}_{13/2})$	0.39±0.06
6.283	10^{-*}	$\nu(1j_{15/2},1i^{-1}_{13/2})$	0.64±0.07
6.437	12^-	$\nu(1j_{15/2},1i^{-1}_{13/2})$	0.46±0.07
6.745	14^-	$\nu(1j_{15/2},1i^{-1}_{13/2})$	0.53±0.04
6.833	$(8^-)^*$	$\pi(1i_{13/2},1h^{-1}_{11/2})$	0.58±0.05
6.859	9^{-*}	$\pi(1i_{13/2},1h^{-1}_{11/2})$	0.55±0.02
6.879	7^{-*}	$\pi(1i_{13/2},1h^{-1}_{11/2})$	0.39±0.01
6.884	10^{-*}	$\pi(1i_{13/2},1h^{-1}_{11/2})$	0.32±0.09
7.064	12^-	$\pi(1i_{13/2},1h^{-1}_{11/2})$	0.32±0.05
7.086	12^{-*}	$\pi(1i_{13/2},1h^{-1}_{11/2})$	0.18±0.02

Conclusions

- Data with unambiguous interpretation point to correlations beyond a mean-field description
  - Elastic nucleon scattering
    - Reaction cross section requires energy dependent imaginary potentials
  - Knock-out cross sections suggest reduction of removal probabilities
    - including fragmentation of single-particle strength indicating imaginary potentials also at energies below the Fermi energy
  - Elastic electron cross section generates charge density that are not explained in detail by mean field approaches
  - Parity violating electron scattering sensitive to neutron skin for N ≠ Z
  - Inelastic electron cross section suggest factors of 2 reductions with respect to mean field results
  - Even level structure around the Fermi energy requires an energy-dependent (real) binding potential —> also requiring an imaginary potential through a dispersion relation (see later)